博士論文番号：1081012

Research of regulation by *S*-nitrosylation of protein post-translation modification in xylem vessel formation

（道管形成におけるタンパク質 *S*-ニトロシル化修飾に関する研究）

Harunori Kawabe

Graduate School of Biological Sciences Nara Institute of Science and Technology (NAIST)

Laboratory of Plant Metabolic Regulation
Supervisor: Professor Taku Demura

2018/1/12

Table of contents

1. Introduction

1-1. *VASCULAR-RELATED NAC DOMAIN* proteins, master regulators of xylem vessel cell differentiation

In vascular plants, the long-distance transport of low-molecular weight compounds, such as water and nutrients, is conducted by xylem vessels. Xylem vessels are composed of a specific type of cell, xylem vessel cell, which can be characterized with the thickened secondary cell wall (SCW) and programmed cell death (PCD). SCW of xylem vessel cells show annular, spiral, reticulate or pitted patterns, and typically contains cellulose, hemicellulose and lignin (reviewed by Fukuda, 2004; Oda and Fukuda, 2012; Schuetz et al., 2013; Kumar et al., 2016). This rigid structure gives the cell strength chemically and physically, resulting in the prevention from cell collapse under the high pressure exerted by fluid uptake. In addition, xylem vessel cells will undergo PCD at maturity (Fukuda, 2004; Turner S., et al., 2007; Escamez and Tuominen, 2014). Through PCD, xylem vessel cells lose all cell contents, and form the hollow structure for water conduction (Supplemental Figure 1). The water conductivity of hollow dead cell is estimated to be higher than that of living cells (Sperry, 2003); thus, PCD is thought to represent a critical innovation required for water conduction cells that developed during early land plant evolution (Xu et al., 2014).

VASCULAR-RELATED NAC DOMAIN1 (*VND1*) to *VND7*, encoding a plant-specific class of NAC transcription factors functioning as key regulators of xylem vessel differentiation, were identified using an inducible xylem vessel cell differentiation system involving *Arabidopsis thaliana* (Arabidopsis) suspension cell cultures (Kubo et al., 2005). All *VND* genes were expressed in developing xylem vessel cells, suggesting the involvement of VND family genes in xylem vessel cell differentiation (Kubo et al., 2005; Yamaguchi et al., 2008). Additionally, the overexpression analysis showed that *VND6* and *VND7* have the ability to induce the ectopic differentiation of metaxylem-type and protoxylem-type vessel cells, i.e. the cells with pitted patterned SCW and helical patterned SCW, respectively (Kubo et al., 2005).

The strong induction activity of VND6 and VND7 for xylem vessel cell differentiation has permitted researchers to discover their downstream factors that function in xylem vessel cell formation (Ohashi-Ito et al., 2010; Zhong et al., 2010; Yamaguchi et al., 2011). These studies successfully identified a lot of genes directly regulated by VND6 and/or VND7, including the genes for PCD and for SCW. These include *MYB46*, *MYB83*, and *MYB103*, encoding the R2R3-type MYB transcription factors that upregulate SCW polymer biosynthetic enzymes, such as *IRREGULAR XYLEM (IRX1)*/*CesA8*, *IRX5*/*CesA4*, encoding SCW-specific cellulose synthase proteins, and *XYLEM CYSTEINE PEPTIDASE 1 (XCP1)*, *XCP2*, and

METACASPASE9 (MC9), the genes involved in PCD (Supplemental Figure 2; Ohashi-Ito et al., 2010; Zhong et al., 2010; Yamaguchi et al., 2011). These data suggested that the VND proteins can induce whole set of genes required for xylem vessel cell differentiation directly or indirectly, as the master regulators of xylem vessel cell differentiation (reviewed by Zhong and Ye 2015; Nakano et al., 2015).

1-2. Transcriptional regulation of VND7 expression

Previous data also indicated that VND6 and VND7 can directly upregulate several transcription factors, such as LOB domain transcription factors, *ASYMMETRIC LEAVES2* (*AS2*)*-LIKE11 (ASL11)/LATERAL ORGAN BOUNDARIES DOMAIN15* (*LBD15)* and *ASL19/LBD30* (Ohashi-Ito et al., 2010; Zhong et al., 2010; Yamaguchi et al., 2011). ASL19/LBD30, as well as LBD18/ASL20, were shown to induce ectopic SCW deposition through the upregulation of *VND6* and *VND7* (Soyano et al., 2008). Interestingly, all VND proteins possess the transactivation activity for the promoter of VND7 expression (Zhou et al., 2014; Endo et al., 2015). These positive transcriptional feedback systems would effectively induce the VND activity to define the xylem vessel cell differentiation during xylem development (Soyano et al., 2008; Nakano et al., 2015).

Recently, VND7 expression was reported to be regulated by multiple classes of transcription factors, including NAC, LBD/ASL, HD-ZipIII and GATA transcription families (Endo et al., 2015). These transcription factors can upregulate VND7 expression in the transient expression assays, however, the overexpression of the putative upstream factors did not induce the VND7 expression *in planta* (Endo et al., 2015), suggesting the possibility that VND7 could be additionally regulated by epigenetic mechanisms. In turn, the VND activity should be tightly regulated by multilayered transcriptional regulation.

1-3. Post-translational regulation of VND7 activity

In addition to the transcriptional regulation of *VND* genes as mentioned above, it is possible that the VND proteins would be subjected to post-translational regulation. The NAC proteins are known to form homo-dimers and/or heterodimers with other NAC proteins (Ernst et al., 2004). Indeed, the VND proteins, the subgroup of NAC family proteins, were shown to form homo-dimers and/or heterodimers within VND family proteins; VND7 can form the heterodimers with VND1-VND6, and the homodimers with VND7 itself, whereas VND6 can only make homo-dimers (Yamaguchi et al., 2008). Moreover, the yeast two hybrid screening identified the VND INTERACTING 2 (VNI2) protein, another NAC protein, as an interactor of VND7 to negatively regulate the VND7 activity (Yamaguchi et al., 2010).

Yamaguchi et al. (2008) also showed a possibility that the VND7 protein is phosphorylated based on the shifted bands of YFP-tagged VND7 protein. The YFP-tagged VND7 protein experiments additionally indicated that VND7 is under the active control of proteasome-based protein degradation (Yamaguchi et al., 2008). These pieces of information implied the critical roles of post-translational regulation of protein activity for xylem vessel cell differentiation, however, the detailed roles for post-translational protein modification are still unclear during xylem vessel cell differentiation.

1-4. Protein *S*-nitrosylation, a post-translational protein modification linked to cell nitric oxide (NO)-related redox states

Currently, our understanding of post-translational protein modification is rapidly expanding (Wang et al., 2014; Snider and Omary, 2014; Skelly et al., 2016). One such protein modification, *S*-nitrosylation, is a reversible modification involving covalent binding between nitric oxide (NO)-related species and a cysteine residue (Jaffrey et al., 2001). NO is known to be generated in cells by NO synthase that converts L-arginine and oxygen to L-citrulline and NO, or by the breakdown of nitrite or other compounds, and NO functions as a reactive nitrogen species (Wendehenne et al., 2001). Efficiency of *S*-nitrosylation is dependent on conditions of NO, oxygen, hydrophobicity, and redox surrounding the targeted cysteine (Marino et al., 2010), and it is coupled with cellular antioxidant redox enzymatic systems (Liu et al., 2001; Benhar et al., 2009; Foster et al., 2009). Thus *S*-nitrosylation is considered to be an important regulatory system for the direct reflection of cellular redox states to protein activities (Spoel et al., 2010; Gupta, 2011).

The majority of *S*-nitrosylation research has been conducted in animal cells, indicating the involvement of *S*-nitrosylation in many aspects of cellular functional regulation (Benhar et al., 2009; Gould et al., 2013). Recently, examples of NO signaling regulating protein activities through the *S*-nitrosylation have increased in plants. For example, the *S*-nitrosylation of specific cysteine residue can inhibit the functions of Open Stomata 1 (OST1)/ Sucrose nonfermenting 1 (SNF1)-related protein kinase 2.6 (Wang et al. 2015). A basic leucine zipper transcription factor, ABI5, the central hub of ABA signaling is also the target of *S*-nitrosylation (Albertos et al., 2015). Moreover, NO signaling mediated by protein *S*-nitrosylation can affect phytohormone signaling, by competing with phosphorylation of *Arabidopsis thaliana* histidine phosphotransfer proteins (Feng et al., 2013). Similarly, enhancement of interaction between the auxin receptor TRANSPORT INHIBITOR RESPONSE 1/AUXIN SIGNALING F-BOX (TIR1/AFB) and auxin response transcription factors AUX/IAAs through *S*-nitrosylation of TIR1/AFB can modulate auxin signaling (Terrile et al., 2012). These increasing lines of

evidence suggest that protein *S*-nitrosylation has critical roles in multiple aspects of cell function and activity in plants.

1-5. Large-scale *S*-nitrosylation proteomics with the mutant of *S-NITROSOGLUTAHIONE REDUCTASE* (*GSNOR*)

The extent of *S*-nitrosylation of any protein will depend on the balance between rates of nitrosylation and denitrosylation. Although *S*-nitrosothiols are generally considered to be labile entities, *S*-nitrosylation reactions are not spontaneously reversible (Supplemental Fig. 3; Hogg, 2002); instead, denitrosylation is thought to be actively regulated by specific enzymes (Zaffagnini et al., 2013; Kneeshaw et al., 2014). One of these enzymes, the denitrosylase *S*-NITROSOGLUTATHIONE REDUCTASE (GSNOR), was originally described as GSH-dependent formaldehyde dehydrogenase, a member of the class III alcohol dehydrogenase family (Benhar et al., 2009). GSNOR reduces *S*-nitrosoglutathione (GSNO), an important donor molecule of NO group for the protein *S*-nitrosylation, but does not act on *S*-nitrosylated proteins directly (Liu et al., 2001). Therefore, it is hypothesized that GSNOR functions in the regulation of protein *S*-nitrosylation by affecting the equilibrium between *S*-nitrosylated proteins and GSNO, to maintain the homeostasis of cellular *S*-nitrosothiols (Feechan et al., 2005; Frungillo et al., 2014; Gong et al., 2015).

In the Arabidopsis genome, only one copy of *GSNOR* gene, *GSNOR1,* is recognized (Xu et al., 2013). Notably, the loss-of-function mutant of *GSNOR1* was reported to be as auxin-impaired, suggesting critical roles for GSNOR1 for plant development and environmental responses (Shi et al., 2015). Currently, a large-scale, proteomic analysis of *S*-nitrosylated Arabidopsis proteins was performed with the wild type and *gsnor1-3* mutant (Hu et al., 2015). The proteomic analysis with the wild type and *gsnor1-3* seedling samples identified 1,195 endogenously *S*-nitrosylated peptides in 926 proteins (Hu et al., 2015). In accordance with the report that NO level is increased in *gsnor1* mutant (Feechan et al., 2005), the number of identified *S*-nitrosylated peptides were larger in *gsnor1-3* than in wild type (Hu et al., 2015). Especially, the proteomics data showed that the proteins related to chlorophyll metabolism and photosynthesis were enriched in the list of *S*-nitrosylation target proteins, and indeed, *gsnor1-3* exhibited the decrease of chlorophyll content and the altered photosynthetic properties (Hu et al., 2015). These findings indicated that the protein *S*-nitrosylation regulated by GSNOR has a great impact on plant cell differentiation and function (Yun et al., 2011; Lin et al., 2012).

1-6. Forward genetic screen suggests GSNOR influences VND7-mediated xylem development.

In the present study, I tried to identify novel regulators of VND7 activity through forward genetic approach with the Arabidopsis VND7 inducible system (*35S::VND7-VP16-GR*) (Yamaguchi et al., 2010). In this system, VND7 is expressed as a fused protein with the transcriptional activation domain of the herpes virus VP16 protein, and a rat glucocorticoid receptor domain, which promotes the protein's translocation into the nucleus under dexamethasone treatment. Upon the glucocorticoid treatment, the VND7 activity was strongly and effectively induced, resulting in almost all the cells of *35S::VND7-VP16-GR* plants becoming transdifferentiated into ectopic xylem vessel cells (Yamaguchi et al., 2010). To isolate novel mutants related to the regulation of VND7 activity, the transgenic Arabidopsis carrying *35S::VND7-VP16-GR* was mutagenized with ethyl methanesulfonate. The screening of mutant pools was performed to isolate suppressor mutants that did not differentiate ectopic xylem vessel cells. Among the obtained lines, the recessive mutant line *suppressor of ectopic vessel cell differentiation induced by VND7-1* (*seiv1*) showed the inhibition of ectopic xylem cell differentiation especially in the above-ground organs. Molecular cloning of the responsible gene for *seiv1* mutation revealed that the phenotypes of *seiv1* were attributed to the loss-of-function mutation of *GSNOR1*. This research led me to propose the novel hypothesis that the GSNOR-based regulation of protein *S*-nitrosylation has critical roles in xylem vessel cell differentiation.

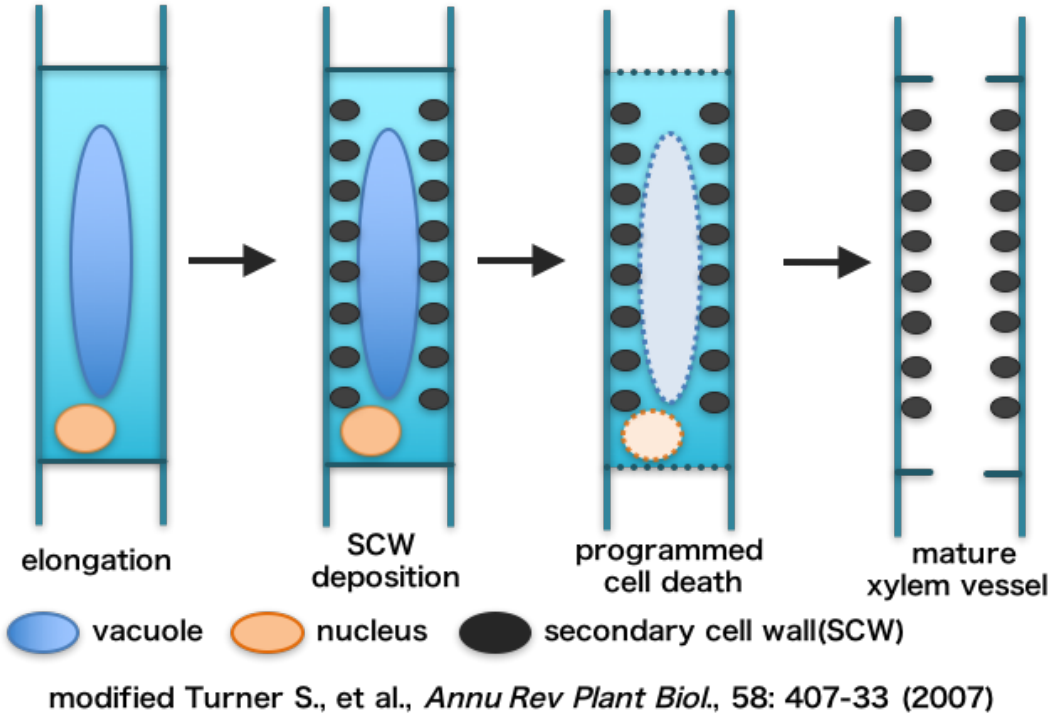

Supplemental Figure 1. Schematic model of xylem vessel differentiation

Xylem vessels differentiation undergo secondary cell wall deposition and programmed cell death. The collapse of the vacuole is a trigger of programmed cell death, and cysteine proteases and other hydrolases are released to carry out autolysis of xylem vessel elements.

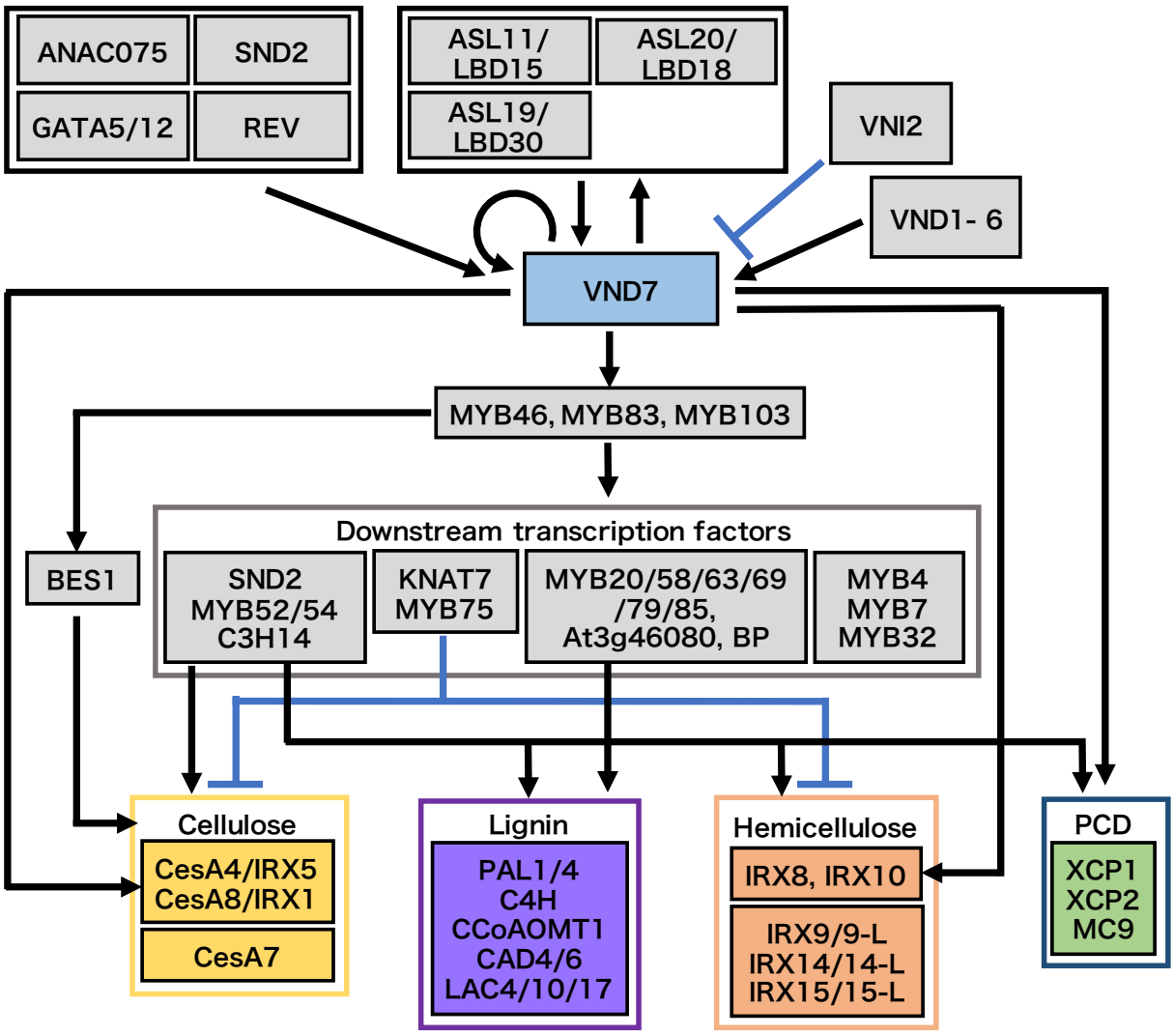

Supplemental Figure 2. Schematic diagram of the transcriptional regulation network of VND7 during xylem vessel differentiation.

VND7 can directly upregulate several transcription factors, such as MYBs (MYB46, MYB83, and MYB103) and LOB domain (ASL11/LBD15 and ASL19/LBD30) transcription factors. Several functional gene families, including the cellulose synthesis, such as CesA4/IRX5 and CesA8/IRX1 genes, the hemicellulose synthesis (IRX8 and IRX10), and the related to the programmed cell death genes (XCP1, XCP2, and Metacaspase 9 (MC9)) are directly regulated by VND7. Recent study indicated that GATA family members (GATA5 and GATA12), and other NAC proteins (ANAC075 and SND2) as upstream factors of VND7.

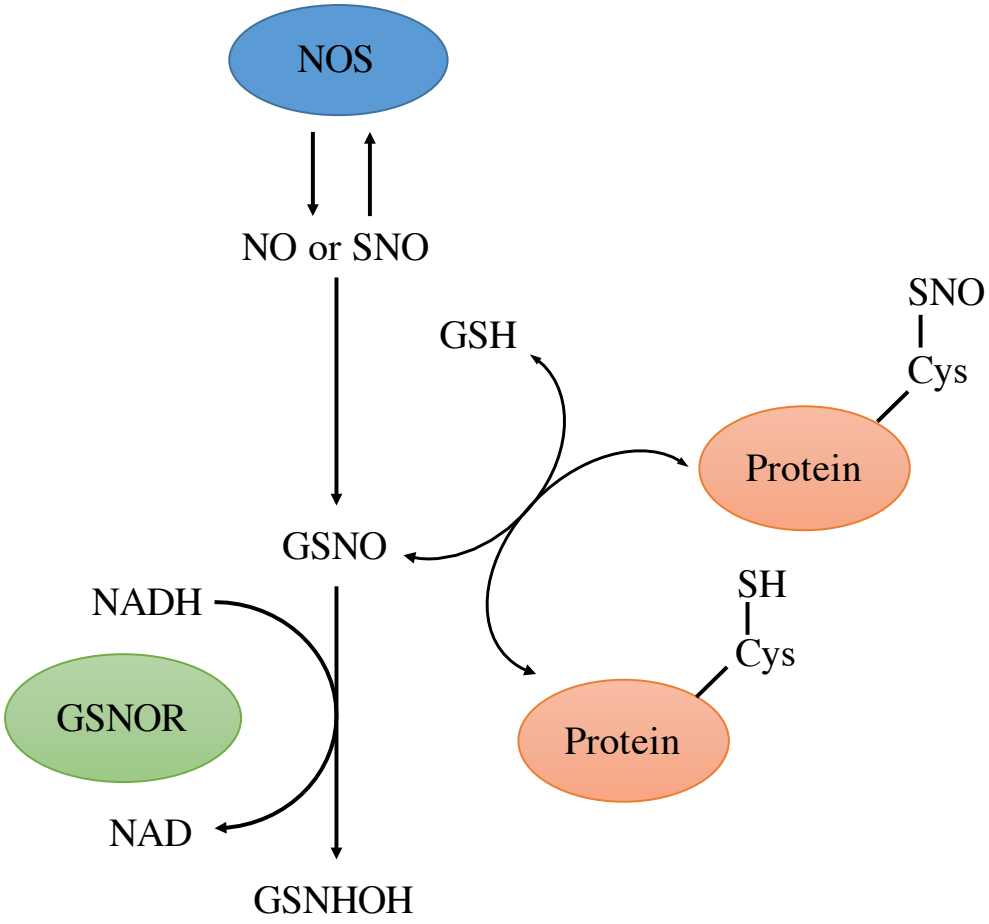

Supplemental Figure 3. Current model of GSNOR-based reversible protein *S*-nitrosylation reaction

S-nitrosylated protein (SNO protein) can be denitrosylated by the transnitrosylation reaction between glutathione (GSH) and *S*-nitrosylated cysteine residue. GSNOR reduces *S*-nitrosoglutathione (GSNO) with NADH, forming *N*-hydroxysulphenamide (GSNHOH) and NAD. Thus, GSNOR can decrease the level of *S*-nitrosylated protein by promoting transnitrosylation from *S*-nitrosylated cysteine residue to GSH, through affecting the equilibrium between GSH and GSNO.

2. Materials and methods

2-1. Plant materials and growth conditions

The *35S::VND7-VP16-GR* and *35S::VP16-GR* (vector control) *Arabidopsis thaliana* (Arabidopsis) plants were described in Yamaguchi et al. (2010). The *seiv1* line, which was generated by the ethylmethane sulfonate-mutagenesis of wild type *35S::VND7-VP16-GR*, was provided from Dr. Misato Ohtani (NAIST, Japan). The *gsnor1-3* mutant (Feechan et al. 2005) was kindly provided by Dr. Loake (University of Edinburgh).

Seeds were surface-sterilized with 0.2% (v/v) PPM™ solution (Plant Cell Technology), and then sowed on the agar-solidified Murashige and Skoog plates [MS salt (Wako Pure Chemical), 1% (w/v) sucrose, 0.5 g/l MES, and 0.6% (w/v) agar, pH5.7]. The plates with seeds were incubated at 4°C for 2-4 days, followed by the transfer to the incubator at 22°C under the continuous light condition. For long-term culture of plants, the plants grown on plates for 2-3 weeks were transferred in the soil, and cultured in the growth chamber at 22°C with a photoperiod of 16 h light and 8 h dark.

2-2. DEX treatment to induce ectopic xylem vessel cell differentiation

The induction of ectopic xylem vessel cell differentiation was performed according to the methods in Yamaguchi et al. (2010). Briefly, 7-day-old seedlings were treated with dexamethasone (DEX), a synthetic glucocorticoid, via the addition of 10 μM DEX solution. The treated plants were incubated for 1 day (for expression analysis) or for 4 days (for histological observation) at 22°C under continuous light condition.

2-3. Plasmids constructions

For the complementation analysis of *seiv1* with the *GSNOR1* gene, the genomic sequence of *GSNOR1* gene including the 818 bp-upstream region was amplified by PCR, using the genomic DNA derived from wild Col-0 Arabidopsis as the template, and then cloned into the pENTR/D/TOPO vector (Invitrogen) according to the manufacturer's instructions. The *GSNOR1* genomic fragment was then transferred into the Gateway destination vector pBG (Kubo et al., 2005) with the LR Clonase (Invitrogen) to generate the GSNOR1(WT)/pBG plasmid.

For the expression of Maltose-binding protein (MBP)-VND7 fusion proteins in *Escherichia coli*, the coding sequence of VND7 cloned in the pENTR/D/TOPO vector (Invitrogen) was transferred in to the Gateway destination vector pMAL-GWRFC (Yamaguchi et al., 2011) with the LR Clonase (Invitrogen).

Mutagenesis of cysteine residues of VND7 protein was performed based on the site-directed, ligase-independent mutagenesis (SLIM) primer design (Chiu et al., 2004), which contains 3 steps of 1) DNA amplification by PCR with the primers targeting nucleotide mutations to lead to the amino acid substitution, 2) PCR mixture digestion by *Dpn*I, 3) Denaturation at 99°C for 3 min, followed by hybridization by two cycles of 65°C for 5 min and 30°C for 15 min. *E. coli* was transformed with the resultant aliquot to obtain the mutagenized plasmids.

For PCR amplification, *pyrobest*™ DNA polymerase (TaKaRa Bio) was used. The primer information used here was described in Table 1.

2-4. Plant transformations

The GSNOR1(WT)/pBG plasmid were introduced into *Agrobacterium tumefaciens* strain GV3101::pMP90 by electroporation. The resultant transgenic *Agrobacterium* was used for the transformation of heterozygous *seiv1* plants by the floral dip method (Clough and Bent 1998). Transgenic seedlings were obtained by screening for antibiotic-resistant seedlings, and established transgenic homozygous *seiv1* plant lines, *seiv1*/ GSNOR1(WT).

2-5. Histological observations

To observe ectopic xylem vessel cells, the mock- or DEX-treated seedlings were fixed in 90% (v/v) acetone for 2 h to 2 d. The samples were washed with 100 mM phosphate buffer (pH 7.2) at least three times, and then incubated in ethanol series for water absorption, and mounted in a clearing solution (8 g of chloral hydrate, 1 mL of glycerol, and 2 mL of water). For venation patterns, cotyledons were fixed in the fixative solution (ethanol: acetic acid [3:1]) for 1 h at room temperature. After the washing by 70% ethanol, samples were incubated in 100% ethanol at 4°C overnight. The samples were then mounted in the clearing solution.

DIC images were obtained with the light microscope (BX51; Olympus) and photographed with a digital DP70 camera (Olympus). The vein observations were performed under dark-field optics (Olympus).

2-6. Genome DNA extraction

To clone the genomic fragment of *GSNOR1*, 11-day-old wild-type Arabidopsis seedlings (Col-0) were subjected to DNA extraction. For Sanger-sequencing of *seiv1*, the cotyledons were collected for DNA extraction. The samples were combined with 20 μl of PrepMan Ultra (Applied Biosystems), boiled for 5 min at 95°C, and diluted 5× with ultrapure water. The resulting samples were used as the genomic DNA samples.

2-7. Quantitative RT-PCR analysis

Quantitative RT-PCR analysis was performed according to the methods described in Yamaguchi et al. (2011). Briefly, for RNA extraction, the seedlings were ground with TissueLyser II (Qiagen). Total RNA was isolated with the RNeasy Plant Mini Kit (Qiagen), according to the manufacturer's instructions. The cDNA synthesis was performed from 1 μg of total RNA using Transcriptor First Strand cDNA Synthesis Kit (Roche). RT-PCR was carried out with LightCycler® 480 DNA SYBR Green (Roche). *UBQ10* was used as an internal control, and the expression values were calculated as the relative values to *UBQ10*. In the case of VND7-downstrem genes, the relative levels for the vector control were shown. The experiments were independently repeated three times.

2-8. Library preparation for whole-genome resequencing analysis

Seven-day-old F_2 seedlings obtained from the crossing between wild type *35S-VND7:VP16:GR* and *seiv1* line were treated by DEX, and the seedlings showing the suppression of ectopic xylem vessel cell differentiation, namely, the homozygous seedling for the *seiv1* mutation were selected. Totally 120 homozygous *seiv1* seedlings were collected and then subjected to genomic DNA extraction for the next generation sequence library preparation. The nuclear fractions were prepared using the "Semi-pure Preparation of Nuclei Procedures" of the CelLytic PN Isolation/Extraction Kit (Sigma-Aldrich) from the bulked 120 seedling samples of wild type *35S-VND7:VP16:GR* and *seiv1*, and then subjected to genomic DNA extraction using a Plant DNeasy mini kit (Qiagen). The genomic DNAs were sheared using Covaris S2 (Covaris) to make 100 bp fragments. Library for deep-sequencing was generated using NEBNext DNA Sample Prep Master Mix Set 1 (New England BioLabs) and Genomic DNA Sample Prep Oligo Only Kit (Illumina).

2-9. Whole-genome resequencing analysis for isolation of single nucleotide polymorphisms (SNPs)

After quality control, the libraries were subjected to deep sequencing on an Illumina Genome Analyzer IIx (Illumina) to obtain 75-bp reads according to the manufacturer's protocol. The raw output data (bcl files) was processed using the bcl2fastq program (Illumina) to obtain sequencing data with quality values (fastq files), and the fastq data from the parental line *35S::VND7-VP16-GR* and *seiv1* were mapped to the TAIR10 reference genome sequence of Arabidopsis (Col-0) using the Bowtie program (v0.12.9; http://bowtie-bio.sourceforge.net/index.shtml) with default parameters. Single-nucleotide polymorphisms (SNPs) between Col-0 and wild-type *35S::VND7-VP16-GR* or between Col-0 and *seiv1* were

detected with Samtools software (v0.1.18; http://samtools.sourceforge.net/). The SNPs were analyzed to identify SNPs located within coding sequences and/or exon-intron junctions using an in-house PERL script.

2-10. Recombinant VND7 protein expression in *E. coli*

Expression of recombinant VND7 protein in *E. coli* was carried out as described in Yamguchi et al. (2011) with slight modifications. The wild type or mutated VND7/pMAL-GWRFC plasmid were introduced into *E. coli* strain Rosetta-gami™ B (DE3) pLysS (Novagen), and the MBP-tagged VND7 protein expression was induced by the culture with 0.1 mM isopropyl β-d-thiogalactopyranoside at 37°C for 4 h. The BMP-VND7 protein was purified with Amylose Resin (New England BioLabs). Protein concentration was checked by Bradford analysis (Zor and Selinger, 1996) with bovine serum albumin as a standard, and the recombinant proteins were purified from the SDS-PAGE gels. Large-scale production of recombinant proteins was carried out as described by Gräslund et al. (2008).

2-11. Biotin switch assay

In vitro S-nitrosylation and subsequent biotinylation of *S*-nitrosylated proteins, called "biotin switch assay" were performed as described by Jaffrey (2001) with some modifications. The experimental condition was optimized with the commercial GAPDH protein (Glyceraldehyde-3-phosphate Dehydrogenase from rabbit muscle, #G2267, Sigma), which is a well-studied *S*-nitrosylated protein, as the positive control. Finally, the optimized condition was determined: the proteins were extracted by a HEN buffer (25 mM HEPES, pH 7.7, 1 mM EDTA, and 0.1 mM neocuproine) and incubated with *S*-nitrosoglutathione (GSNO) for 20 min at room temperature in dark. Then, the proteins were incubated with 30 mM *N*-ethylmaleimide (NEM) and 2.5% (w/v) SDS at 50°C for 20 min, with frequent vortexing, for the blocking of non-nitrosylated free cysteine residues. Residual NEM was removed by precipitation with 4 times volumes of −20°C acetone, and the precipitate proteins were washed with 80% (v/v) acetone at least twice. The proteins were resuspended in 100 μl of HEPES buffer containing 2.5% (w/v) SDS, and subjected to biotinylation by adding 2 mM biotin-HPDP, 50 mM ascorbate, and, 10 μM $CuSO_4$, followed by the 2 h-incubation at RT (Wang et al., 2008). Residual biotin-HPDP was removed by precipitation with 4 times volumes, and the resultant pellets were carefully washed with an additional 80% (v/v) acetone. The proteins were then separated by non-reducing SDS-PAGE, and transferred onto PVDF membranes, for Western blotting analysis using a primary anti-biotin antibody (1: 8,000 dilution ratio; Sigma, #B7653) and an anti-mouse secondary antibody conjugated with peroxidase (1: 20,000 dilution ratio; Sigma, #NA931).

Signals were visualized as the chemi-luminescence signals by Amersham ECL Prime kit (GE Healthcare Life Sciences).

2-12. Transient reporter assay

For transient reporter assay, the protoplast cells were generated from Arabidopsis T87 suspension cultured cells, according to the method of Abel and Theologis (1994) with slight modifications. The T87 cells were treated with the enzyme solution [1% (w/v) cellulase 'Onozuka' RS (Yakult, Tokyo, Japan), 0.05% (w/v) pectolyase Y-23 (Kyowa Chemical), 5 mM EGTA, and 0.4 M mannitol, pH5.6] for 80-90 min, and then filtered with a 40 μm nylon mesh. Protoplasts were collected by the centrifugation (×100 g, 3 min, at room temperature), and diluted in the solution composed of 1 vol. 0.5 M mannitol and 2 vol. 200 mM $CaCl_2$. After the subsequent centrifugation (×100 g, 3 min, at room temperature), the protoplast pellet was resuspended in the solution composed of 2 vol. 0.5 M mannitol and 1 vol. 200 mM $CaCl_2$, followed by the centrifugation (×100 g, 3 min, at room temperature). Finally, the protoplasts were resuspended in 30 ml of W5 solution (154 mM NaCl, 125 mM $CaCl_2$, 5 mM KCl, 5 mM glucose, 1.5 mM MES-KOH, pH 5.6) and incubated on ice for at least 30 min before the transfection.

Protoplasts were resuspended to the density of 5×10^6 protoplasts ml^{-1} in MaMg solution (0.4 M mannitol, 15 mM $MgCl_2$, 5 mM MES-KOH, pH 5.6). A mixture of 10 μl plasmid DNAs containing 500 ng of pAGL-X1E1, 200 ng of the effector plasmids, and 100 ng of *Renilla* luciferase expression plasmid pRL-SV40 (Yamaguchi et al. 2008) was added to 190 μl of protoplast solution, and gently mixed. Immediately the PEG solution (0.4 M mannitol, 100 mM $Ca(NO_3)_2$, 40% (w/v) PEG 4000) was added to make a final PEG concentration of 20% (w/v), and carefully and gently mixed by pipetting. After the 20-min incubation at room temperature, the protoplast mixture was carefully diluted with 1.2 ml of W5 solution, and the protoplasts were collected by the centrifugation (×100 g, 3 min, at room temperature). The protoplasts were washed once with 0.4 M mannitol/W5 solution (4:1), and then resuspended in a 400 μl of modified MS medium (Nagata, 1987) with or without 1 mM *S*-nitrosoglutathione (GSNO). Transfected protoplasts were incubated in the dark at 22°C for 20 h. The luciferase activities were measured by the Dual-Luciferase Reporter Assay System (Promega) and the TriStar LB 941 (Berthold).

Table 1. Primer information used in this study

Primer name	Sequence (5'- 3')
For Site-directed, Ligase-Independent Mutagenesis	
VND7_C58S_F2	GCGAGGAGTAAACTAGGGTATGAAGAGCAAAACGAGTG
VND7_C58S_R2	CCCTAGTTTACTCCTCGCTTGTATATCCCATGGCTC
VND7_C153S_F2	GGCTGGGTGGTGTCTCGAGCATTTAGGAAGC
VND7_C153S_R2	TCGAGACACCACCCAGCCTTCCTCCTGAACC
VND7_C264S_F2	AGCTTTAACTCTGTGGATTGGAGAACACTAGATACC
VND7_C264S_R2	ATCCACAGAGTTAAAGCTCTTCTCTTCTTCTTGCTC
VND7_C320S_F	CATTCTCTTGGAAGCTTCCCTGACTCG
VND7_C320S_R	GAAGCTTCCAAGAGAATGATGAATATTAGC
For qRT-PCR analysis	
CesA4-RT-for1	GAGTGATGATAAAACGATGAGCAG
CesA4-RT-rev1	TCTCAAAATTCTTCTGCGACATTA
CesA7-RT-for1	ATGGGTAGACAGAACAGAACACCAA
CesA7-RT-rev1	CTTCAGCAGTTGATGCCACACTT
CesA8-RT-for1	CACTTCTTTGCCTCTTGTTGCTTAC
CesA8-RT-rev1	GAAGCTCGAGGACACTCGTTAAGAT
endo_VND7_RT_F	aatacgtttataggatcatcgtgg
endo_VND7_RT_R	TTTGATAGTACCGCCTTGTCTCTAC
exo_VND7_RT_F	cttggatgcttccctgactc
exo_VND7_RT_R	gtcctcgccgtctaagtgg
IRX10-RT-for1	GTGAGAAGGCACTGAACTGGACT
IRX10-RT-rev1	GACTTCTAATGTTTTTGAAGTGCT
IRX8-RT-for1	TCAAGAGCTGTCACATTAGAGCAT
IRX8-RT-rev1	ATGATCCGGTAGAGAAGTGAAAAC
LBD30-for4	CTATCTACGGCTGCGTCTCTCACATCGT
LBD30-rev7	TAGAGATCCTGAAGATGACACCGGAAC
MYB046-for2	GAATGTGAAGAAGGTGATTGGTACA
MYB046-rev4	CGAAGGAACCTCAGTGTTCATCA
Ubq10-for1	AACTTTGGTGGTTTGTGTTTTGG
Ubq10-rev1	TCGACTTGTCATTAGAAAGAAAGAGATAA

XCP1-for1	TTGACCCATGAAGAGTTCAAAGGAAGA
XCP1-rev1	GAAAGCGAACTCAGATTCCCTGTTG

For checking the SNPs of whole genome sequencing

At5g39020_F	TGCAAGACCAAATCCAGAACT
At5g39020_R	GCTTAGCAAGGCCAAAGTCG
At5g40320_F	CCTAGTTGAGGAGCTCTCTGACG
At5g40320_R	CCATCCCACACATCCCTCCT
At5g42220_F	CGGGTCATTGGAGCAGTTCT
At5g42220_R	TCTCCATTGCTTCGCTGGTT
At5g42260_F	CCTTGAAGATGCTTATGGAGGGTTCCT
At5g42260_R	CGATAGGCACTCCTTCTCTTTCACCTG
At5g42390_F	GCTTGAGCGTAGTGTCTGGT
At5g42390_R	TACCTTGCCGGGAGTTGAAG
At5g42480_F	TACCCCAAGCAATATTCCAGCAGAGTC
At5g42480_R	CAATAAAGACACCAGGCTCACCATCAC
At5g42850_F	TTGAAGAAGGTGGACGCGAA
At5g42850_R	TGAGCACGAAATCGTAAAGATCA
At5g43940_F	ATCACTTGCAAAGCTGCGGT
At5g43940_R	CAGTCACGAGTTGGAACGGA
At5g44070_F	GAACCTGCGTATTGTGGTTTGGCTAGT
At5g44070_R	TTAAGAGGAACCCAGTGAGGGGGATAC
At5g44080_F	ACGACGGCTTCTGATGTTGT
At5g44080_R	CGTAAAAACCGTGGTGGCTG
At5g45520_F	AGACTCCGACCTGAAGAAGA
At5g45520_R	CTGCAGAATGCACATGAGGC
At5g45560_F	ACCACAGAATCACGATGGCA
At5g45560_R	TGTGAGAACCACTCACGCAA
At5g48100_F	GAATGCGGTAGGTTTTCCCCTTCTCTAC
At5g48100_R	GTGGTCAGATGGTCCTGAATACATCACA
At5g48470_F	TTTCCTCCACACCATCACCTT
At5g48470_R	ATCCGGAATAGCTGGCCTTG
At5g49680_F	TGGCACTGAGAAGCATCCTG
At5g49680_R	CCAGCTCCTGGATCGACATC

Primers for genotyping

At5g43940_HindIII_F	GGTACCTTTATCCTCGATCCTCGCACTCT
At5g43940_HindIII_R	GAGCAGTGTAGAGGATCTTGATCCGAACC
bar_+337_R	ACTTCAGCAGGTGGGTGTAGAG
bar_+88_F	GAGACAAGCACGGTCAACTTCC

For construction of the vectors

TOPO_At5g43940_F	cacctgctaaacctcagcaaaatcatg
TOPO_At5g43940_R	cccaccagaaacctattcatgtgtcct
VND7_CDS_full_F	CACCATGGATAATATAATGCAATCGTC
VND7_CDS_full_R	TTACGAGTCAGGGAAGCATCCAAGAG
pENTR_+1003_R	CCTCGACGTTTCCCGTTGAA
pENTR_+380_F	CCGGCGGATTTGTCCTACTC

Primers for sequence verification of MBP-VND7 vectors

MalE_+618_F	TGCAGACACCGATTACTCCATC
MalE_+988_R	TTTCACCTTTCTGGGCGTTTTC
VND7_CDS_+276_F	CTGGAAAGCCACGGGTAGAG
VND7_CDS_+704_R	AACTGCGGGAGCTCAATGTT

Primers for sequence verification of 35S::VND7-VP16-GR cassette

35S_pro_F1	ACTCATTAGGCACCCCAGGCTTTACACTT
GR_+194_F	TGTTAGGTGGGCGTCAAGTG
GR_+617_R	CCTTCCCTTTTGACGATGGC
GVG_+615_F	TAGCTCTGTTCCAGATTCAGCATGGAG
GVG_+962_R	CAGAGATACTCTTCATAGGATACCTGC
pBI121_+4512_F	GTCGCTACTGATTACGGTGCTGCT
T17F3-60424_R	GCTTCTATTTCCGCGATTGACTTTTGA
VP16_+1279_R	TCGTCTAGCGCGTCGGCATGCGCCATC

3. Results

3-1. Suppressor mutant screening to isolate novel regulatory factors of VND7

Yamaguchi et al. (2010) established the Arabidopsis VND7 inducible line, *35S::VND7-VP16-GR*, in which the transdifferentiation of xylem vessel cells can be induced in almost all types of cells in seedlings by the application of glucocorticoids, such as dexamethasone (DEX) (Fig. 1). In order to isolate novel regulatory factors of VND7 activity, the *35S::VND7-VP16-GR* plants were mutagenized with ethyl methanesulfonate, and the screening of the mutagenized *35S::VND7-VP16-GR* plants was performed previously to isolate suppressor mutants for ectopic xylem vessel cell differentiation (Ohtani et al., unpublished). One of these suppressor mutants is the putative recessive line *seiv1*, in which ectopic xylem vessel cell formation was inhibited, therefore the seedling can survive after the DEX treatment, whereas the wild type *35S::VND7-VP16-GR* seedlings died after the transdifferentiation into xylem vessel cells (Fig. 1). The F_1 plants between *35S::VND7-VP16-GR* and *seiv1* showed the segregation ratio of surviving plants: dead plants = 31 : 87 ($\chi^2 = 0.7498$), indicating that the *seiv1* mutation is a recessive mutation, and that the suppressor phenotype of *seiv1* can be attributed to a single mutation occurred in the *seiv1* genome.

3-2. Suppression phenotype of seiv1 for ectopic xylem vessel cell differentiation

To check the suppression phenotype of *seiv1* for ectopic xylem vessel cell differentiation, 7-day-old seedlings of the wild type *35S::VND7-VP16-GR* and *seiv1*, as well as the vector control, were treated with or without 10 μM DEX for 4 days. In the case of vector control plants, no apparent difference of growth and development was found between seedlings with and without the DEX treatment (Fig. 2A). By contrast, in the wild type *35S::VND7-VP16-GR*, the transdifferentiation into xylem vessel cell occurred in all types of cells by the DEX treatment as previously reported (Fig. 2; Yamaguchi et al., 2010). The patterned secondary cell wall (SCW) depositions were observed in cells of cotyledons, leaves, hypocotyls and roots (Fig. 2B), and the seedlings turned white as the cells underwent PCD (Fig. 2A; Yamaguchi et al., 2010). The *seiv1* seedlings, however, did not show the bleaching after the DEX treatment (Fig. 2A). In the cotyledons and leaves of *seiv1*, the ectopic SCW in mesophyll cells was not observed (Fig. 2B). Similar suppression of ectopic SCW formation was also observed in hypocotyls of *seiv1* (Fig. 2B). Interestingly, the root cells of *seiv1* showed ectopic SCW with helical patterns similar to the wild type *35S::VND7-VP16-GR* (Fig. 2B). These results indicated that the ectopic xylem vessel cell differentiation was strongly suppressed in the above-ground organs in the *seiv1* line.

Of note, the *seiv1* seedlings displayed the severe dwarf phenotype even when they were grown without the DEX treatment (Fig. 2A). The defective growth was observed in *seiv1* throughout its lifetime, implying that the responsible gene for the *seiv1* mutation would have critical molecular functions for plant growth and development.

3-3. Expression analysis of VND7 downstream genes during ectopic xylem vessel cell differentiation

To reveal expression levels of VND7 downstream genes in *seiv1*, I carried out quantitative RT-PCR analysis using total RNA samples prepared from the wild type *35S::VND7-VP16-GR, seiv1*, and the vector control treated with or without 10 μM DEX for 1 day, for SCW-specific cellulose synthase genes, *CesA4*, *CesA7*, *CesA8* (Taylor et al., 2003); biosynthetic genes for hemicellulosic polysaccharide xylan, *IRX8* (Persson et al., 2007) and *IRX10* (Brown et al., 2009); transcription factors *ASL19/LBD30* (Soyano et al., 2008) and *MYB46* (Kim et al., 2013); and the PCD marker xylem-specific cysteine peptidase *XCP1* (Funk et al., 2002; Avci et al., 2008). Even without DEX treatment, the expressions of these VND7 downstream genes were higher in the wild type *35S::VND7-VP16-GR* than those in the vector control (Fig. 3A). The DEX treatment greatly increased the expression of these genes in the wild type *35S::VND7-VP16-GR*, which showed more than 100 times higher levels than those in the vector control (Fig. 3B). In contrast, in the *seiv1* plants, the increase of VND7 downstream gene expressions by the DEX treatment was suppressed; the VND7 downstream genes were upregulated by the DEX treatment, however, the expression levels were 10 times or less than the vector control (Fig. 3B). The suppressed expressions of VND7 downstream genes were also observed in *seiv1* without DEX treatment (Fig. 3A), suggesting that the VND7 activity to induce xylem vessel cell-related genes was affected not only in ectopic xylem vessel cell differentiation, but also in endogenous xylem vessel development in *seiv1*.

I also checked the endogenous and exogenous *VND7* gene expression levels in the wild type *35S::VND7-VP16-GR*, *seiv1* and the vector control plants. The exogenous *VND7*, i.e. the *VND7* gene contained in the chimeric cassette *35S::VND7-VP16-GR,* was driven by strong constitutive *CaMV* 35S promoter. It is important to note that this constitutive expression means that the exogenous *VND7* gene expression is not determined by DEX treatment in the wild type *35S::VND7-VP16-GR* and *seiv1* (Fig. 4A), DEX treatment triggers translocation of the pre-existing VND7-VP16-GR into the nucleus. Consistent with the previous observation that VND7 can upregulate *VND7* expression by itself (Endo et al., 2015), the wild type *35S::VND7-VP16-GR* plants showed the increase of endogenous *VND7* expression after the induction of VND7 activity by the DEX treatment (Fig. 4B). Such upregulation of endogenous *VND7*

expression by the DEX treatment was not observed in *seiv1* (Fig. 4B), as shown in the VND7-downstream genes (Fig. 3B). I also found that the level of endogenous *VND7* expression in *seiv1* was lower than that in the wild type *35S::VND7-VP16-GR* and vector control plants under the mock treatment (Fig. 3B). Therefore, the decreased expression of VND7-downstream genes in *seiv1* under the mock treatment (Fig. 3A) could be attributed to a defect in endogenous *VND7* expression.

3-4. Whole-genome-resequencing analysis to obtain SNP information of seiv1 genome

Next, to identify the responsible gene for the *seiv1* phenotype, whole-genome-resequencing analysis was performed with the genomic DNA samples obtained from the wild type *35S::VND7-VP16-GR* and *seiv1* (Table 2). The sequence data was analyzed with CASAVA pipeline software version 1.7 (Illumina) to detect SNPs among the reference Col-0, the wild type *35S::VND7-VP16-GR*, and *seiv1*. As shown in Table 3, the genome of wild type *35S::VND7-VP16-GR* and *seiv1* possessed 4,087 and 4,748 SNPs, respectively. To narrow down SNPs related to the *seiv1* phenotype, the SNPs commonly found in wild type *35S::VND7-VP16-GR* and *seiv1* were removed, resulting in the detection of 712 SNPs in the *seiv1* genome (Fig. 5). Finally, I selected 15 SNPs in 15 genes as these homozygous SNPs are predicted to result in amino acid substitution (Table 4). These SNPs were all located in Chromosome 5, with the substitution from C/G to T/A, as expected for the EMS mutagenesis (Table 4). Resequencing of these SNPs by Sanger sequencing methods verified all the 15 SNPs in *seiv1*.

3-5. *seiv1* exhibits similar phenotypes with *S-nitrosoglutathione reductase 1* mutant

The list for genes with *seiv1*-specific SNPs contained 15 genes whose mutants have been reported (Table 4). One of them is *AT5G43940* encoding the *S*-nitrosoglutathione reductase 1 (GSNOR1) protein, the mutants of which are known as *gsnor1-3* (Feechan et al., 2005), *paraquat resistant 2* (*par2-1*) (Chen et al., 2009), or *sensitive to hot temperatures 5* (*hot5*) (Lee et al., 2008). The fact that loss-of-function mutants of AT5G43940 showed severe growth defects similar to *seiv1* (Fig. 2A) directed me to check whether *seiv1* shares other phenotypes found in *gsnor1* mutants. First, I examined the paraquat resistance phenotype reported in *par2-1*, in which the missense mutation made the GSNOR1 protein unstable (Chen et al., 2009). In the presence of paraquat, the wild type *35S::VND7-VP16-GR* and vector control arrested the seedling development (Fig. 6A), whereas *seiv1* showed greening cotyledons with paraquat (Fig. 6A), indicating that *seiv1* is a paraquat resistant mutant. Additionally, previous studies indicated that *gsnor1-3*, *hot5*, and *par2-1* mutants had higher levels of NO species than those in the wild-type plants (Feechan et al., 2005; Lee et al., 2008; Chen et al., 2009). Thus, I also analyzed the

intracellular NO level in *seiv1* by the staining with 4,5-diaminofluorescein diacetate (DAF-2DA), a fluorescent dye for *in vivo* imaging of NO (Lee et al., 2008; Chen et al., 2009). The DAF-2DA fluorescent signals in the vector control roots were at undetectable levels, however, the DAF-2DA signals were apparent in both of the wild type *35S::VND7-VP16-GR* and *seiv1*, suggesting that the introduction of *35S::VND7-VP16-GR* cassette could increase the NO level (Fig. 6B). Importantly, the DAF-2DA signals in *seiv1* roots seemed to be higher than those in the wild type *35S::VND7-VP16-GR* roots, especially in the central cylinder regions (Fig. 6B). Thus the strong DAF-2DA signal indicates that NO level are increased in *seiv1*, consistent with the phenotype described for the loss-of-function mutants of *GSNOR1* (Feechan et al., 2005; Lee et al., 2008; Chen et al., 2009).

3-6. *GSNOR1* is a responsible gene for *seiv1* phenotypes

The *gsnor1*-related phenotypes of *seiv1* described above strongly suggested that *seiv1* is a *gsnor1* mutant allele. To check this possibility, the complementation test of *seiv1* by the wild-type *GSNOR1* genomic fragment was performed. The *seiv1* seedlings carrying the wild-type *GSNOR1* genomic fragment recovered the bleaching phenotype typically observed after the DEX treatment in the wild type *35S::VND7-VP16-GR* (Fig. 7A). Moreover, the dwarf phenotype of *seiv1* was also rescued by the introduction of the wild-type *GSNOR1* genomic fragment into *seiv1* (Fig. 7B). These data indicated that the responsible gene for the *seiv1* mutant phenotypes, the suppression of ectopic xylem vessel cell differentiation and growth defects, is *GSNOR1*. In the *seiv1* genome, a G-to-A transition was found in the second exon of *GSNOR1* (Fig. 8A), and the substitution of glutamic acid residue at the 36th position into lysine residue (E36K) would result in *seiv1* (Fig. 8B). The glutamic acid residue at the 36th position is contained in the catalytic domain of GSNOR (Kubienová et al., 2013), and highly conserved among GSNOR of plant, animal, and bacteria (Fig. 8B). *seiv1* was shown to be a recessive mutant, which could be rescued by the wild-type copy of GSNOR1, and its phenotypes were similar to those of reported loss-of-function *GSNOR1* mutants, therefore the E36K missense mutation in *seiv1* represents a novel loss-of-function mutant allele of GSNOR1.

3-7. Loss-of-function mutations of GSNOR1 affect endogenous xylem vessel formation

The results of expression analysis of VND7 downstream genes showed that the expression levels of xylem vessel cell-related genes were decreased in *seiv1* mutants, even without DEX treatment (Fig. 3), suggesting that *gsnor1* mutations affect endogenous xylem vessel cell differentiation. To check this possibility, the venation of 7-day-old cotyledons of the vector control, wild type *35S::VND7-VP16-GR*, *seiv1* and *gsnor1-3* were observed. In the vector

control and wild type *35S::VND7-VP16-GR*, the typical venation pattern where secondary veins branch from the mid-vein to form four loops without gaps (pattern 5; Fig. 9) was the majority. By contrast, in *seiv1* and *gsnor1-3*, the venation patterns 6 to 8, which are not found in the vector control and wild type *35S::VND7-VP16-GR*, were detected. The patterns 6 and 7 had disconnected veins (15.4% of *seiv1* and 34.7% of *gsnor1-3*), and the pattern 8 contained vascular islands (13.9 % of *seiv1* and 4.1% of *gsnor1-3*) (Fig. 9). These data indicated that the *gsnor1* mutations affect endogenous xylem vessel formation.

In *gsnor1-3*, after the increased intracellular NO level, the enhancement of protein *S*-nitrosylation was reported (Hu et al., 2015). The increased NO level in *seiv1* (Fig. 6B) suggested the possibility that similar enhancement of protein *S*-nitrosylation might be linked to the suppression of ectopic xylem vessel cell differentiation in *seiv1*. Thus, I compared two gene lists, the list of known *S*-nitrosylated Arabidopsis protein (in total 932 genes; Hu et al., 2015; Terrile et al., 2012; Albertos et al., 2015; Wang et al., 2015; Tada et al., 2008; Feng et al., 2013) and the combined list of VND7-downstream genes and VND7-interacting protein genes (in total 488 genes; Yamaguchi et al., 2011; Zhong et al., 2010; Yazaki et al., 2016). Comparison of these lists indicated that 6 genes encoding BETA GLUCOSIDASE 18 (BGLU18), RIBULOSE BISPHOSPHATE CARBOXYLASE SMALL CHAIN (RBCS) 1A, RBCS2B, ALANINE:GLYOXYLATE AMINOTRANSFERASE 1 (AGT1), NITRILE SPECIFIER PROTEIN 1 (NSP1), and METACASPASE 9 (MC9) were *S*-nitrosylated VND7-related genes. Among them, the roles for *S*-nitrosylation of MC9, a developing xylem-specific protease, in xylem vessel cell differentiation was well characterized; the *S*-nitrosylation repressed the MC9 activity by the inhibition of self-processing (Belenghi et al., 2007). This implied that the repression of MC9 activity by enhanced *S*-nitrosylation could be one of reason why xylem vessel cell differentiation was affected in *seiv1*.

3-8. VND7 protein can be *S*-nitrosylated *in vitro*

In *seiv1*, the induction of all the tested VND7-downstream genes by the DEX treatment appeared to be defective (Fig. 3B). These findings prompted the hypothesis that *S*-nitrosylation of VND7 protein could be important for its function. To test this idea, I carried out a biotin-switch assay (Jaffrey et al., 2001) with the rabbit muscle GAPDH protein (#G2267, Sigma) as a positive control (Galli et al., 1998), and MBP-MCS protein as a negative control. The recombinant VND7 protein tagged with maltose-binding protein (MBP) (MBP-VND7) was expressed in *E. coli* (Fig. 10). After the optimization of experimental conditions to avoid possible false-positive results in the biotin-switch assay (Fig. 11A, B, C; Wang et al., 2008), the MBP-VND7 was subjected to the biotin-switch assay. The anti-biotin antibodies gave a positive

signal in the presence of the NO-carrier *S*-nitrosoglutathione (GSNO), but not with glutathione alone (GSH) (Fig. 11D), indicating that VND7 protein can be received *S*-nitrosylation.

It is known that *S*-nitrosylation occurs at cysteine residues, thus I next examined which cysteine residues in VND7 protein can be targeted for *S*-nitrosylation. The VND7 protein possessed 4 cysteines, Cys-58, Cys-153, Cys-264 and Cys-320 (Fig. 12A). The Grantham polarity plot analysis (http://web.expasy.org/protscale/), with a window size of nine amino acids, indicated that the Cys-264 and Cys-320 were surrounded by polar amino acids in an environment with a high electrostatic potential, suggesting the Cys-264 and Cys-320 are in a favorable environment for *S*-nitrosylation. In contrast, the environment of Cys-58 and Cys-153 are characterized by a low electrostatic potential (Fig. 12B), which is less likely to be favored for *S*-nitrosylation. To test these predictions, the substitutions of cysteine residues to serine residues were introduced into the recombinant VND7 protein by the Site-directed, Ligase-Independent Mutagenesis (SLIM) method (Chiu et al., 2004). For each of the four possible *S*-nitrosylation sites, each of the other available Cys were mutated to a Ser, e.g. *S*-nitrosylation of C58 was tested with the C153S/C264S/C320S triple mutant protein. When C264 and C320 were the only available sites, a positive signal was found in the biotin-switch assay (Fig. 12C). In contrast, the substitutions of both of Cys-264 and Cys-320 eliminated the *S*-nitrosylated signals (Fig. 12C), clearly indicating that the Cys-264 and Cys-320 of VND7 protein were targets for *S*-nitrosylation.

3-9. Transactivation activity of VND7 is affected by the mutations of Cys-264 and Cys-320

I also tested effects of increased NO level and of substitutions of Cys-264 and Cys-320 on transcriptional activation activity of VND7 by a transient reporter assay. The chimeric genes of *XCP1 (X1E1) pro::LUC*, in which the firefly Luciferase gene was fused with the *XCP1* promoter fragment X1E1 (the promoter region of –148 to –96 bp sufficient to interact with VND7, Yamaguchi et al. 2011) was used as the reporter (Fig. 13A). As the effectors, *35S::VND7* containing the coding region of wild type VND7 (WT) or mutated VND7, which has substitutions of Cys-264 and/or Cys-320 into Ser or Trp (single mutants of C264S, C320S, C264W, and C320W, and double mutants of C264S/C320S and C264W/C320W), fused with the *CaMV 35S* promoter were used (Fig. 13A). The plasmids containing these fusion genes were co-introduced with the reference *35S::RLUC* plasmid into protoplast cells derived from Arabidopsis cultured cells, by the polyethylene glycol-based method (Abel and Theologis, 1994).

The luciferase activity of wild type VND7 (WT) was more than 140 times larger than that of the control (*35S::MCS*) under mock culture condition (Fig. 13B). Notably, in the presence

of GSNO in the culture medium, the luciferase activity activated by the wild type VND7 (WT) was half the value of mock conditions (Fig. 13B). Similar decrease in the control effector (*35S::MCS*) suggested that the increased NO level could also affect basal levels of gene expression. I next examined the transactivation activities of mutant VND7. As a result, it was indicated that all mutations of Cys-264 and/or Cys-320 to Ser or Trp, which were expected to mimic non-*S*-nitrosylated or *S*-nitrosylated forms of VND7, respectively, decreased the luciferase activity compared with the wild type VND7 (Fig. 13C), suggesting the importance of Cys-264 and Cys-320 residues for the regulation of VND7 transactivation activity.

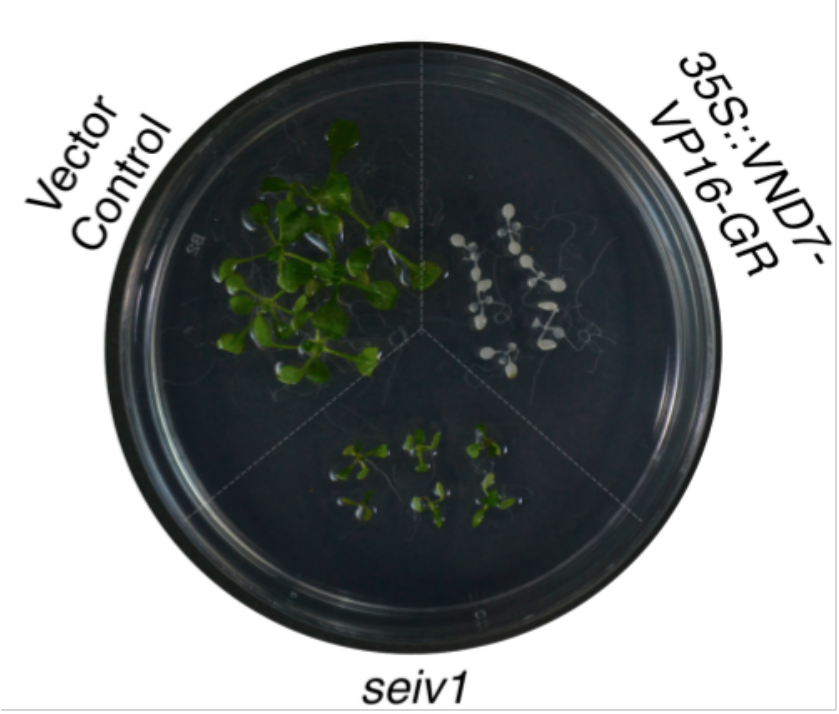

Figure 1. The *seiv1* line is the novel suppressor mutant for ectopic xylem vessel cell differentiation

Seven-day-old seedlings of the vector control, wild type *35S:VND7-VP16-GR*, and heterozygous *seiv1* were treated by dexamethasone (DEX) for 4 days. In the wild type *35S:VND7-VP16-GR*, all cells were transdifferentiated into xylem vessel cells by the DEX treatment, thus the *35S:VND7-VP16-GR* seedlings were died and bleached.

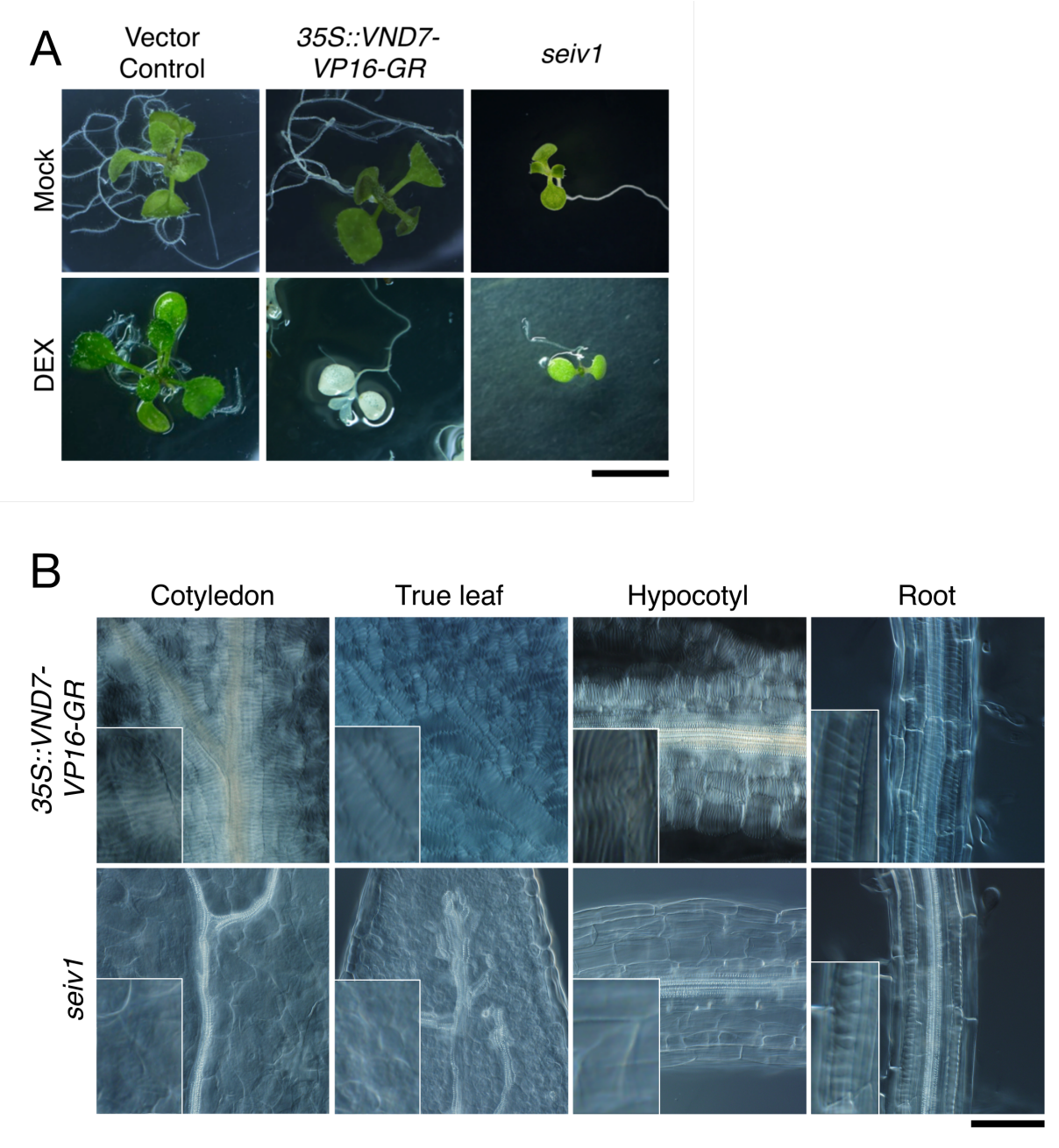

Figure 2. Ectopic xylem differentiation under DEX treatment was suppressed in *seiv1* seedlings

(A) Seven-day-old seedlings of the vector control, wild type *35S:VND7-VP16-GR*, and *seiv1* were treated with (+DEX) or without (-DEX) dexamethasone (DEX) for 4 days. Scale bar = 5 mm.

(B) Microscope observations of DEX-treated wild type *35S:VND7-VP16-GR* and *seiv1*. Insets indicated close-up views of cells with xylem vessel cell-specific helical patterned secondary cell wall in all organs of wild type *35S:VND7-VP16-GR* and roots of *seiv1*. Such patterned secondary cell wall was not observed in upper-ground tissues of *seiv1*. Scale bar = 100 μm.

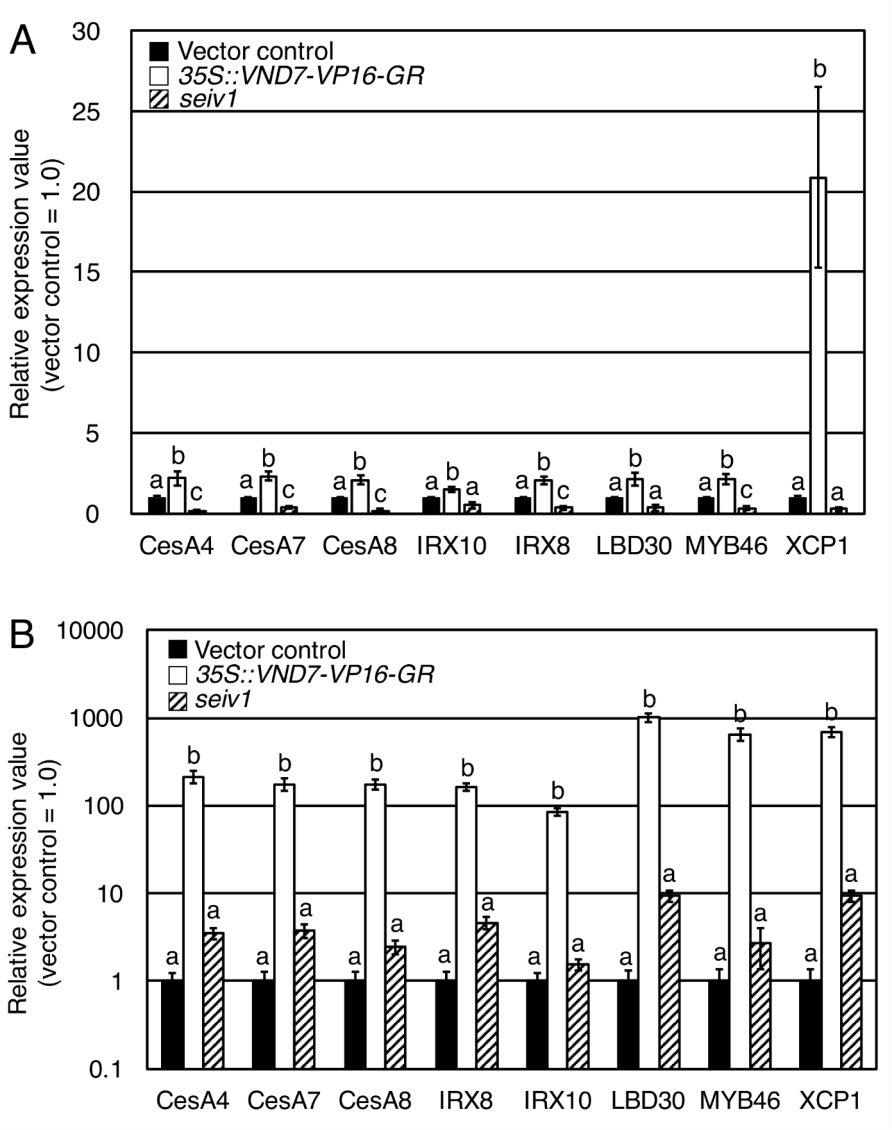

Figure 3. Expression analysis of VND7 downstream genes with or without DEX treatment
Seven-day-old seedlings of the vector control, wild type *35S:VND7-VP16-GR*, and *seiv1* were treated by dexamethasone (DEX) for 1 day, and subjected to the total RNA extraction. Expression levels of SCW-specific cellulose synthase genes, *CesA4*, *CesA7*, *CesA8*, biosynthetic genes for hemicellulosic polysaccharide xylan, *IRX8* and *IRX10*, transcription factors *ASL19/LBD30* and *MYB46*, and xylem-specific cysteine peptidase *XCP1,* which function in the downstream of VND7, were examined by quantitative RT-PCR analysis. The *UBQ10* gene was used as the internal control, and relative values for the vector control results were shown (i.e. the values of vector control samples were set as 1.0). Results were shown as means ± SD (n = 3). Different letters indicate statistically significant differences ($P<0.05$, Tukey's test).

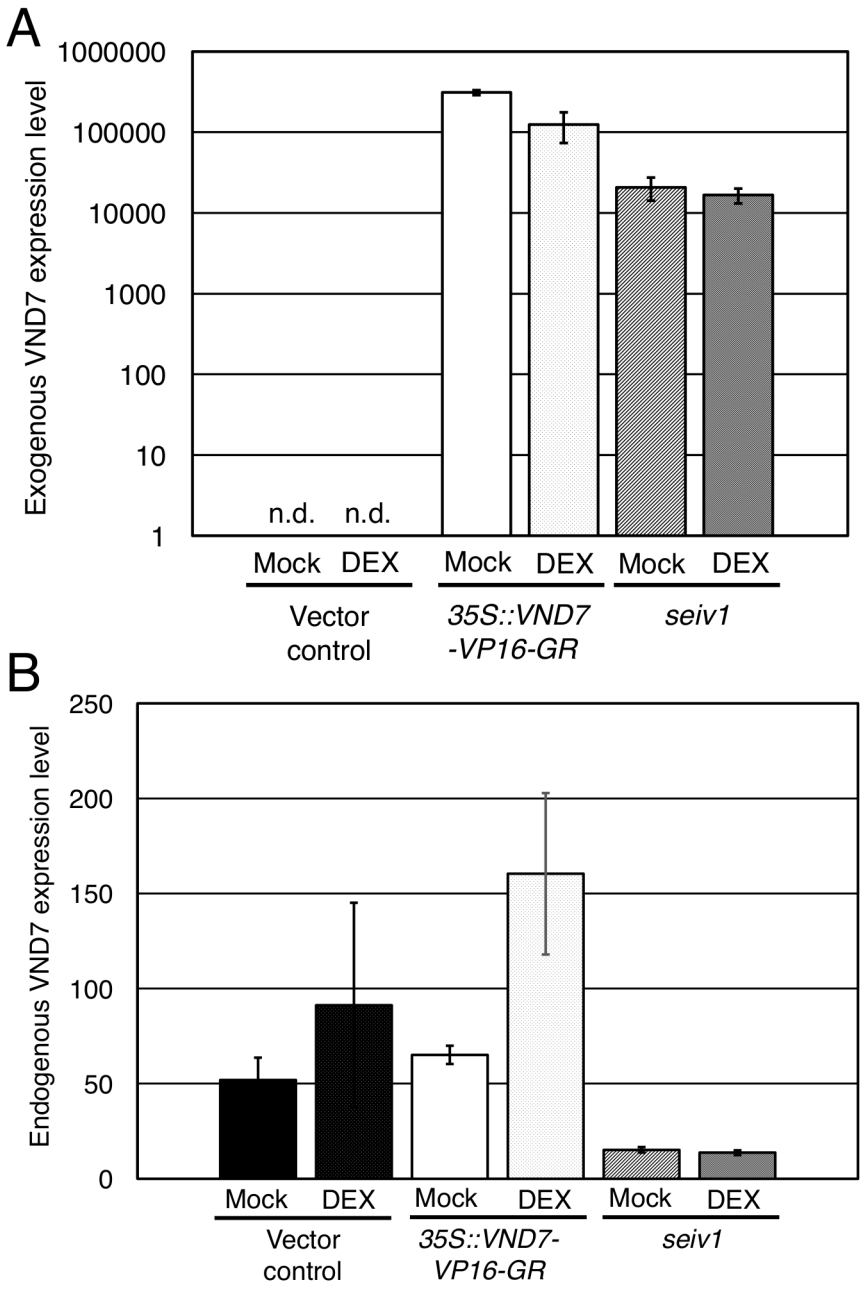

Figure 4. Expression analysis of endogenous and exogenous *VND7* genes with or without DEX treatment

Seven-day-old seedlings of the vector control, wild type *35S:VND7-VP16-GR*, and *seiv1* were treated by dexamethasone (DEX) for 1 day, and subjected to the total RNA extraction. Expression levels of endogenous (A) and exogenous (B) *VND7* expression levels were examined by quantitative RT-PCR analysis. The *UBQ10* gene was used as the internal control, and relative values. Results were shown as means ± SD (n = 3). n.d. = not detected.

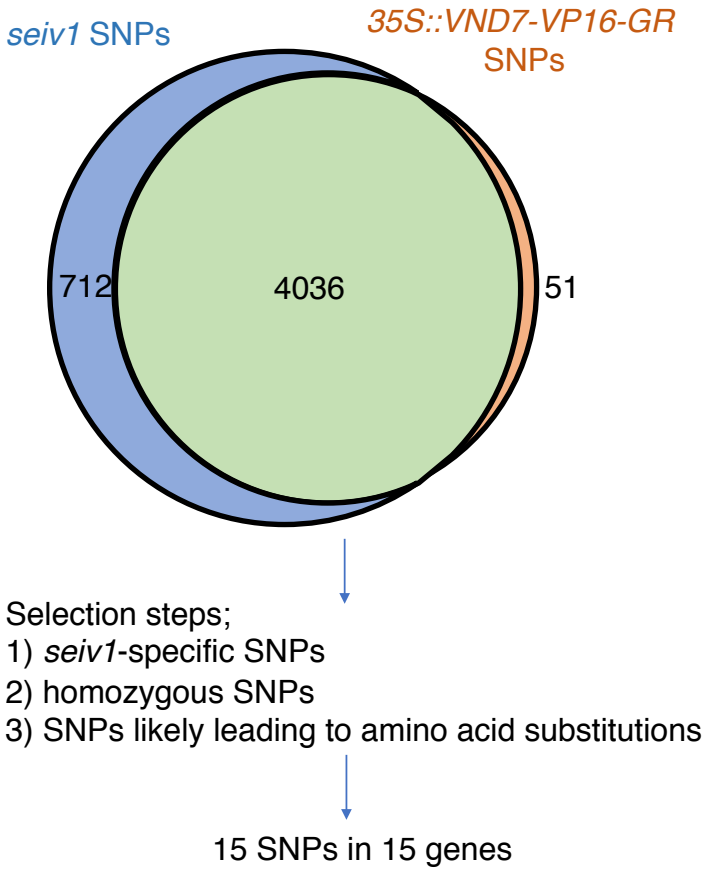

Figure 5. Screening of detected single nucleotide polymorphisms for isolation of responsible genes for *seiv1* mutation

Whole-genome-resequencing analysis showed the genomes of wild type *35S:VND7-VP16-GR* and of *seiv1* possess 4087 and 4748 single nucleotide polymorphisms (SNPs) against the Col-0 genome, respectively. After selection steps of 1) *seiv1*-specific SNPs, 2) homozygous SNPs, 3) SNPs expected to bring amino acids substitution, I obtained 15 SNPs in 15 genes as the candidate for *seiv1* mutation.

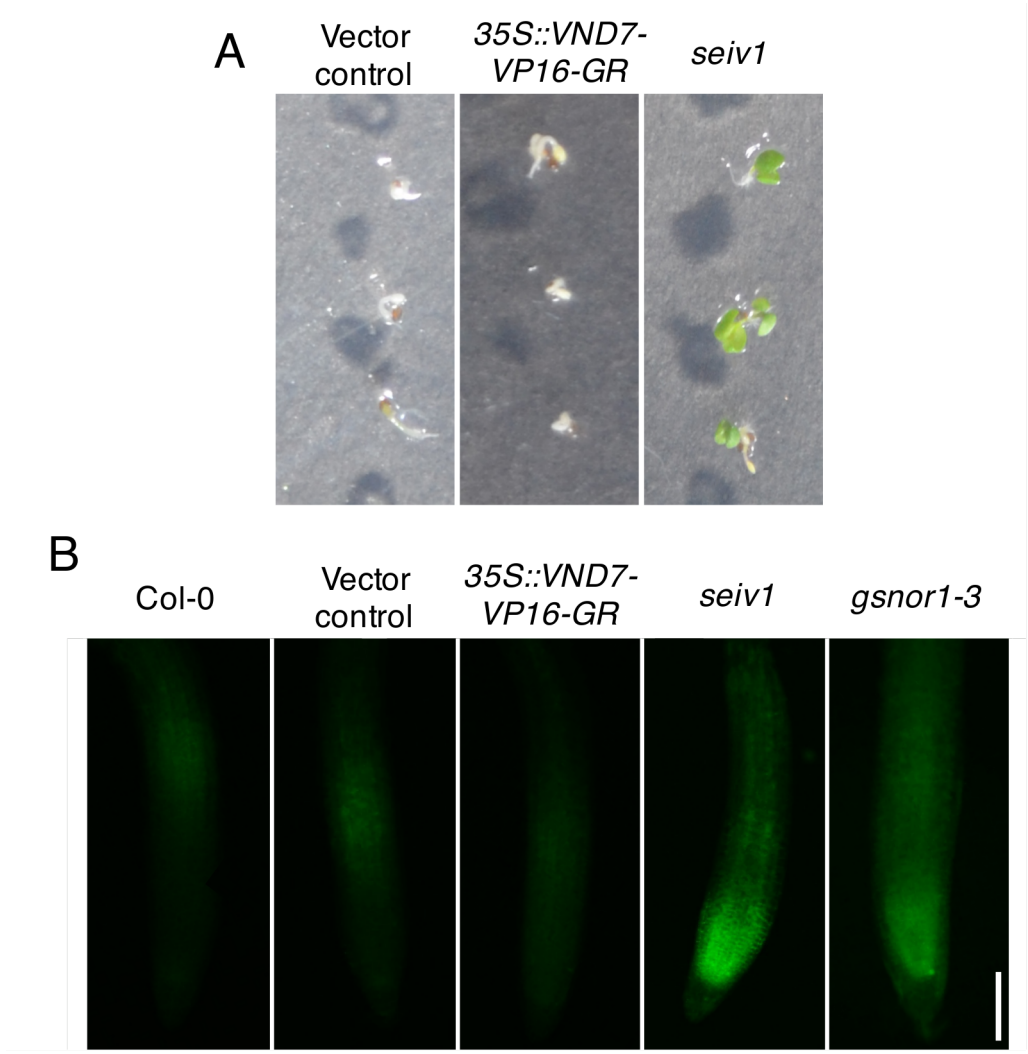

Figure 6. The *seiv1* line showed paraquat tolerance and high nitric oxide (NO) level

(A) Vector control, *35S::VND7-VP16-GR*, and *seiv1* seedlings were grown on MS medium containing 2 μM paraquat for 7 days.

(B) Increased nitric oxide contents in seiv1 roots. Seven-day-old wild type (Col-0), vector control, *35S::VND7-VP16-GR*, *seiv1*, and *gsnor1-3* seedlings were germinated and grown on MS medium, followed by staining with DAF-2DA. Roots were observed and photographed under a fluorescence microscope. Bar = 200 μm.

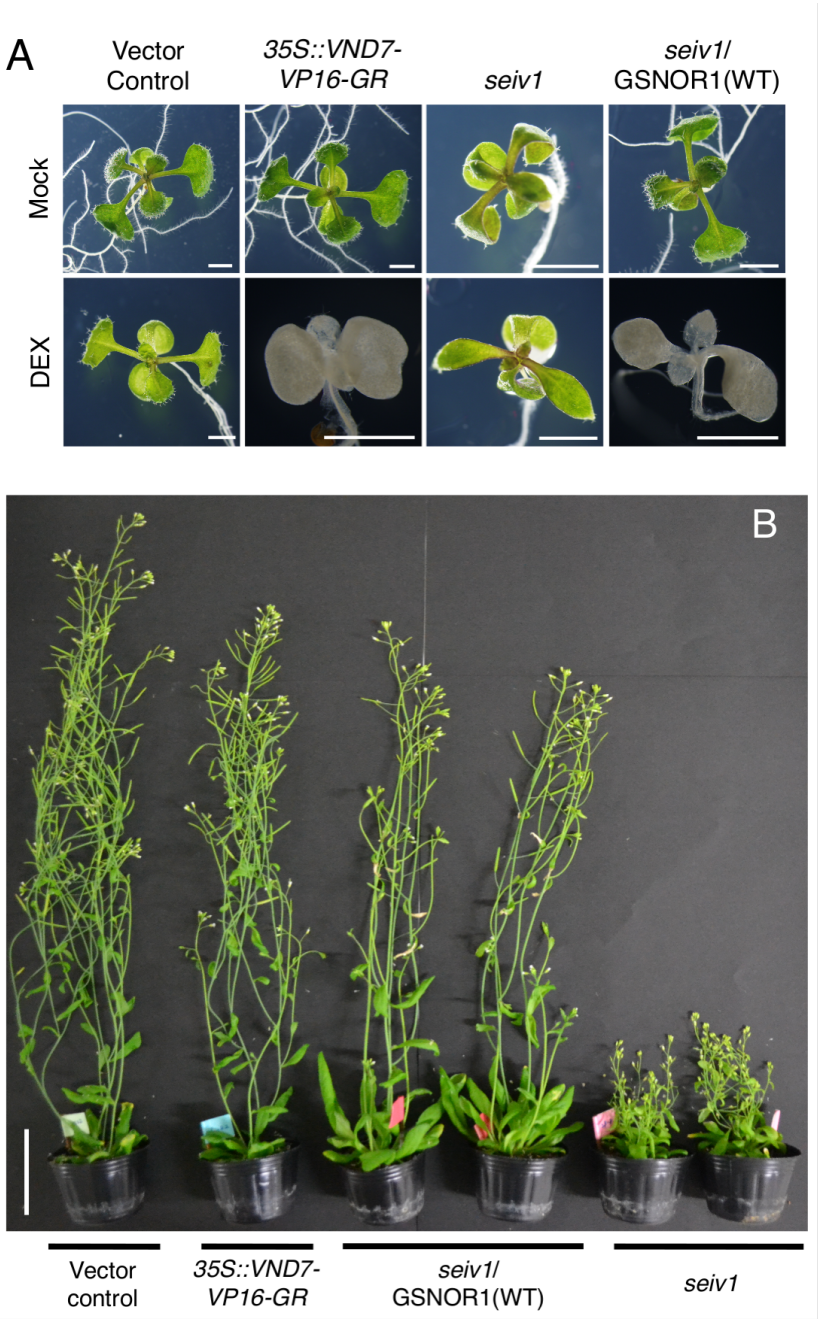

Figure 7. Introduction of wild type *S-NITROSOGLUTATHIONE REDUCTASE 1* (*GSNOR1*) gene complemented *seiv1* phenotypes

(A) Seven-day-old vector control, wild-type *35S::VND7-VP16-GR*, and *seiv1*/*GSNOR1*(WT), (*seiv1* carrying wild-type *S-NITROSOGLUTATHIONE REDUCTASE 1* [*GSNOR1*]) seedlings treated with dexamethasone (DEX) for 4 days. Scale bar = 2 mm.

(B) Vector control, wild-type *35S::VND7-VP16-GR*, seiv1/*GSNOR1*(WT), and *seiv1* plants (42 days old). Scale bar = 5 cm.

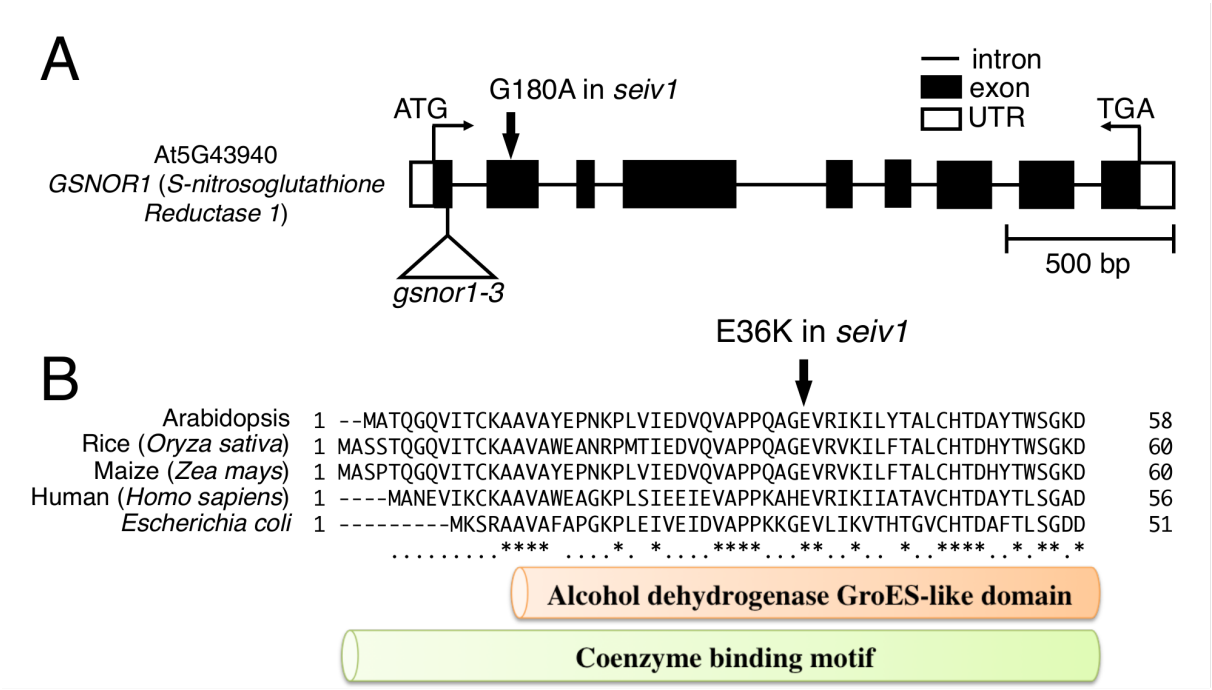

Figure 8. Mutation in *S-NITROSOGLUTATHIONE REDUCTASE 1* (*GSNOR1*) gene in the *seiv1* genome

(A) Gene structure of *S-NITROSOGLUTATHIONE REDUCTASE 1* (*GSNOR1*) (At5g43940). In the *seiv1* genome, single nucleotide substitution, G180A, was occurred. T-DNA insertion position in the reported loss-of-function mutant allele, *gsnor1-3*, was shown.

(B) Partial amino acid sequences of GSNOR1 of Arabidopsis, rice (*Oryza sativa*), maize (*Zea mays*), human (*Homo sapiens*) and *E. coli* (*Escherichia coli*). The single nucleotide substitution in *seiv1* was expected to change the conserved 36th glutamic acid (E), which locates in the region annotated as alcohol dehydrogenase-like domain and coenzyme binding motif, to lysine (K) residue.

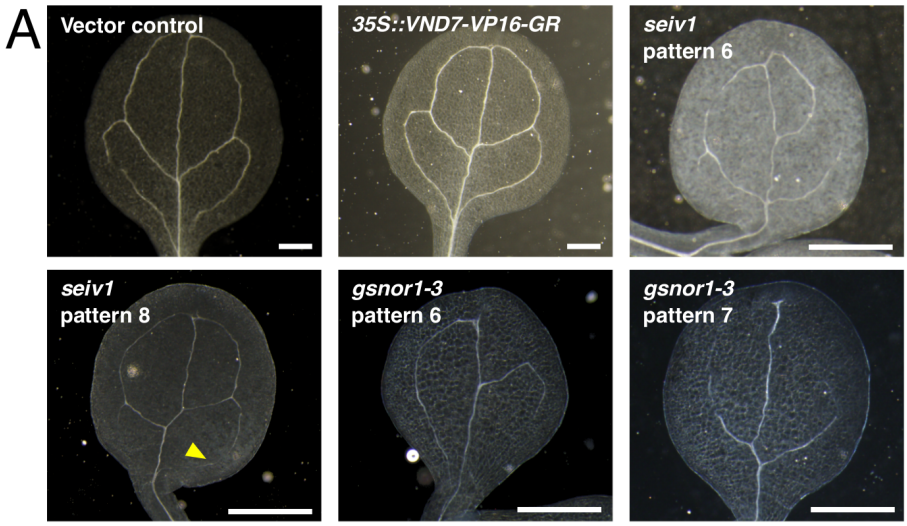

B

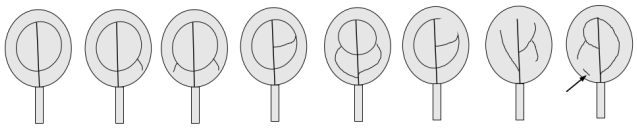

Line	n	Venation patterns							
		1	2	3	4	5	6	7	8
vector control	54	1	6	13	9	25	0	0	0
35S::VND7-VP16-GR	45	0	3	4	4	34	0	0	0
seiv1	65	6	15	10	11	4	10	0	9
gsnor1-3	49	13	5	6	6	0	12	5	2

Figure 9. Veination patterns in cotyledons of *seiv1* and *gsnor1-3*

(A) Typical images of seven-day-old cotyledons of the vector control, wild type *35S:VND7-VP16-GR*, *seiv1*, and *gsnor1-3*. Categories of patterns were indicated in (B). Yellow arrowhead indicated "vascular islands" phenotype. Scales = 2 mm.

(B) Variations of venation patterns observed in the vector control, wild type *35S:VND7-VP16-GR*, *seiv1*, and *gsnor1-3*. Arrow in the drawing for pattern 8 indicated "vascular islands".

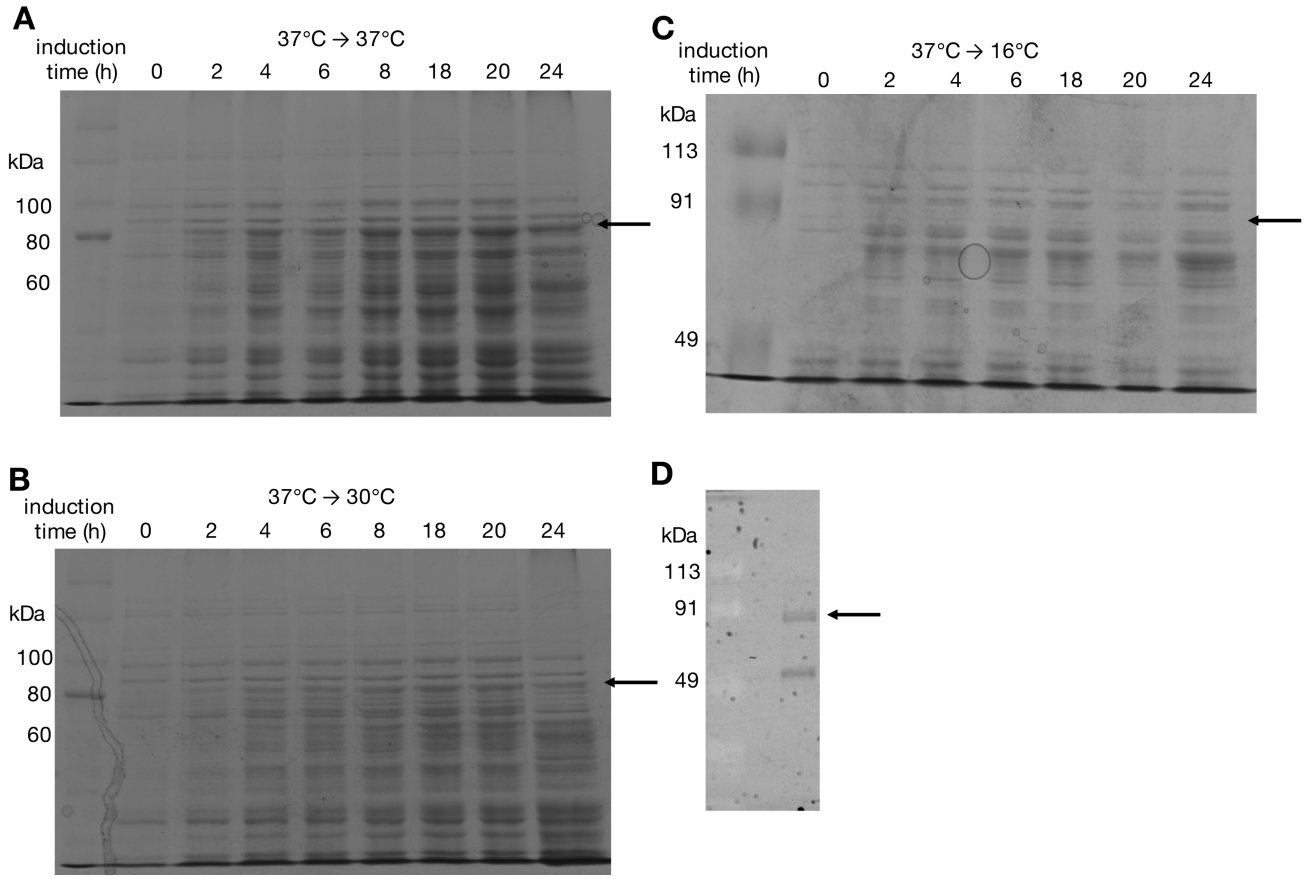

Figure 10. Expression and purification of recombinant MBP-VND7 protein.

(A)-(C) Optimization of incubation temperature condition for the recombinant MBP-VND7 protein in *E. coli* strain Rosetta gami B (DE3) pLysS. Pre-culture of transgenic *E. coli* was performed at 37°C, and then the induction of the MBP-VND7 expression was induced by the addition of 0.1 mM IPTG at 37°C (A), 30°C (B), and 16°C (C).

(D) Purified MBP-VND7 protein by the amylose resin was detected by the UV crossink methods using TGX Stain-Free™ FastCast™ Acrylamide Kits (Bio-Rad). Arrows indicated the expected size of MBP-VND7 (79.9 kDa).

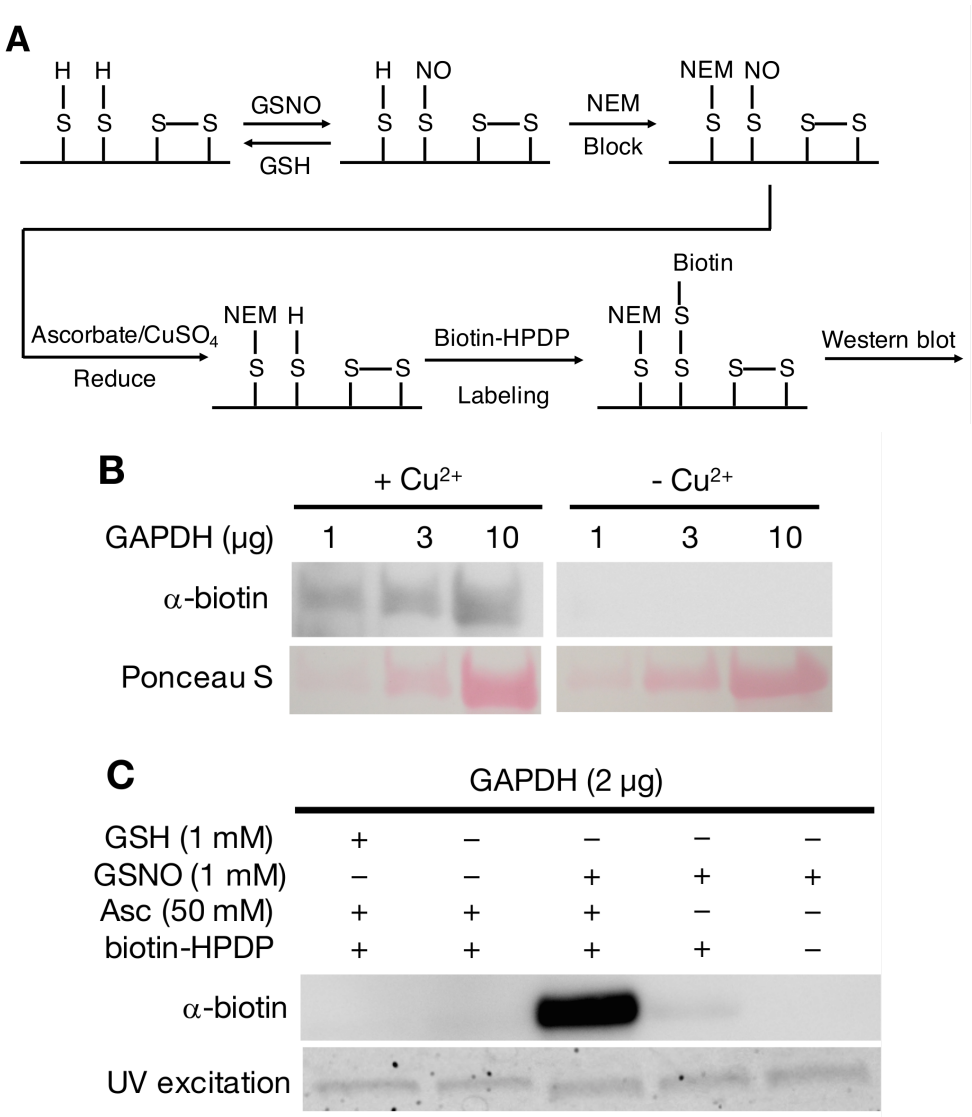

Figure 11. MBP-VND7 protein can be *S*-nitrosylated *in vitro*

(A) Biotin-switch assay to detect *S*-nitrosylation of protein.

(B) and (C) Optimization of biotin-switch assay using the recombinant GAPDH protein, which is the known protein with *S*-nitrosylation modification. (A) Effects of pre-treatment with 20 μM $CuSO_4$ to reduce *S*-nitrosylated protein on the biotin-switch signals. The $CuSO_4$ treatment ($+Cu^{2+}$) increased the biotin-switch signals of GAPDH (see "α-biotin" panel), whereas no biotin-switch signal was detected without the $CuSO_4$ treatment ($-Cu^{2+}$), indicating the requirement of reducing agent before the biotin-switch assay. Inputs were shown by Ponceau S staining. (C) After the pre-treatment of 20 μM $CuSO_4$, the biotin-switch assay was carried out with and/or without the indicated chemical components.

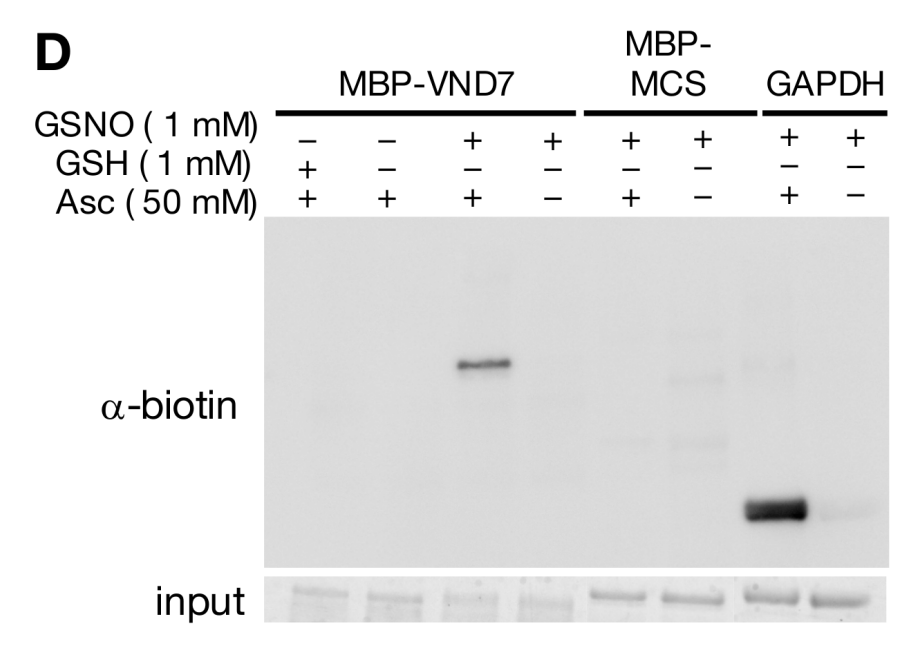

Figure 11. Continued

(D) The 2 μg of MBP-VND7, MBP-MCS (negative control), GAPDH (positive control) were subjected to the biotin-switch assay. The signals to indicate *S*-nitrosylation were detected for MBP-VND7 and GAPDH.

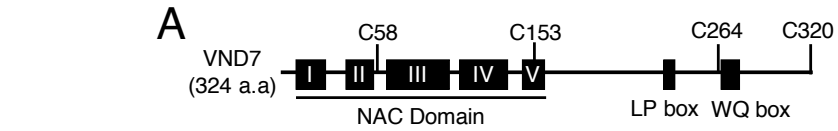

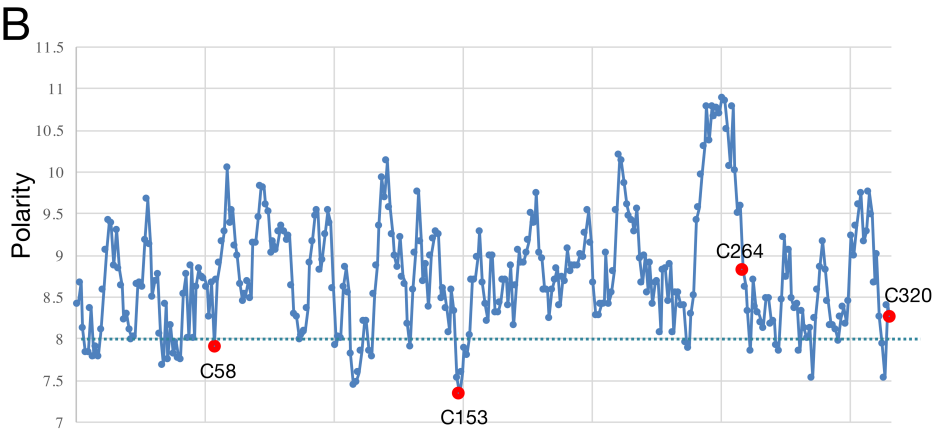

Cystein position	Polarity (Grantham plot)
C58	7.911
C153	7.333
C264	8.622
C320	8.267

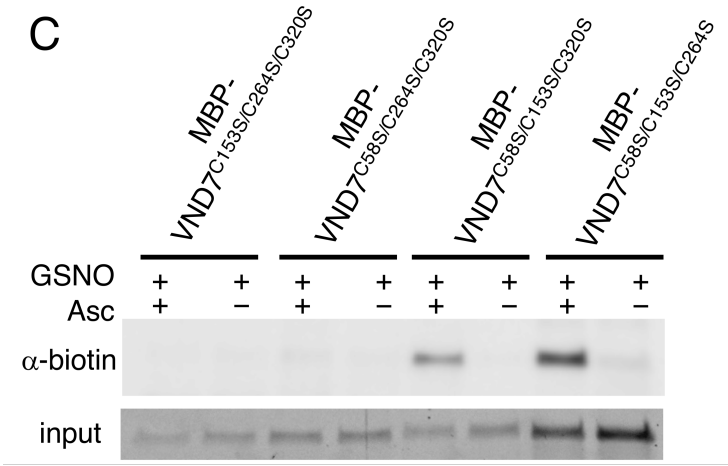

Figure 12. Residues of Cys-264 and Cys-320 of VND7 were targeted for *S*-nitrosylation

(A) Four cysteine residues found in the VND7 protein.

(B) Polarity plot of the VND7 protein by using grantham polarity plot analysis http://web.expasy.org/protscale)

(C) Mutant MBP-VND7 protein series with substitutions of cysteine (C) to serine (S) were subjected to the biotin-switch assay. Signals were detected in the proteins with Cys-264 or Cys-320, indicating that these 2 cysteine residues can be *S*-nitrosylated *in vitro*.

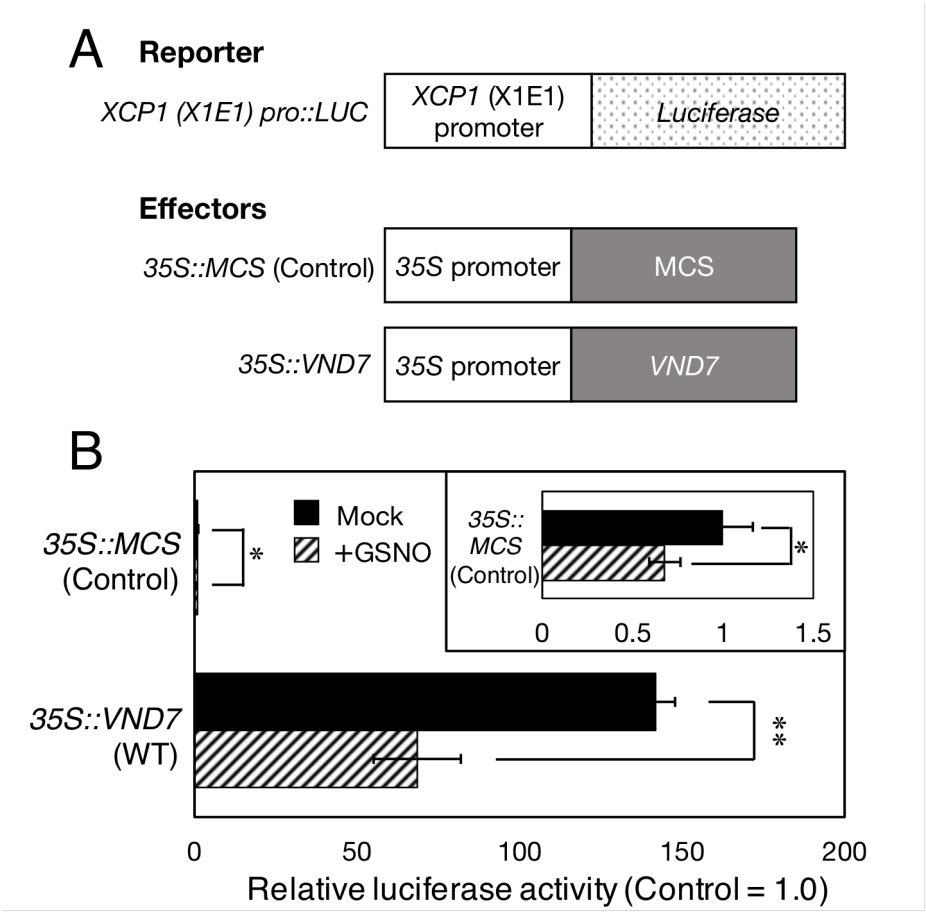

Figure 13. Effects of the mutations of Cys-264 and Cys-320 on transactivation activity of VND7.

(A) Schematic diagrams of reporter and effector plasmids used in transient reporter assay. The reporter plasmid *XCP1 (X1E1) pro::LUC* contains the firefly luciferase gene fused with the *XCP1* promoter fragment X1E1 (the promoter region of –148 to –96 bp, Yamaguchi et al. 2011). The effector plasmid *35S::VND7* contains the coding sequences of wild type VND7 (WT) or mutated VND7 (C264S, C320S, C264S/C320S, C264W, C320W, or C264W/C320W) fused with the *CaMV 35S* promoter. For the control effector, the multi-cloning site (MCS) sequence was fused with the *CaMV 35S* promoter.

(B) Result of transient reporter assays to test effects of *S*-nitrosoglutathione (GSNO) application. The reporter gene activity was normalized with the activity of Renilla luciferase. Asterisks indicate statistically significant differences (Welch's t-test; *$P < 0.05$, **$P < 0.01$) between with and without GSNO application.

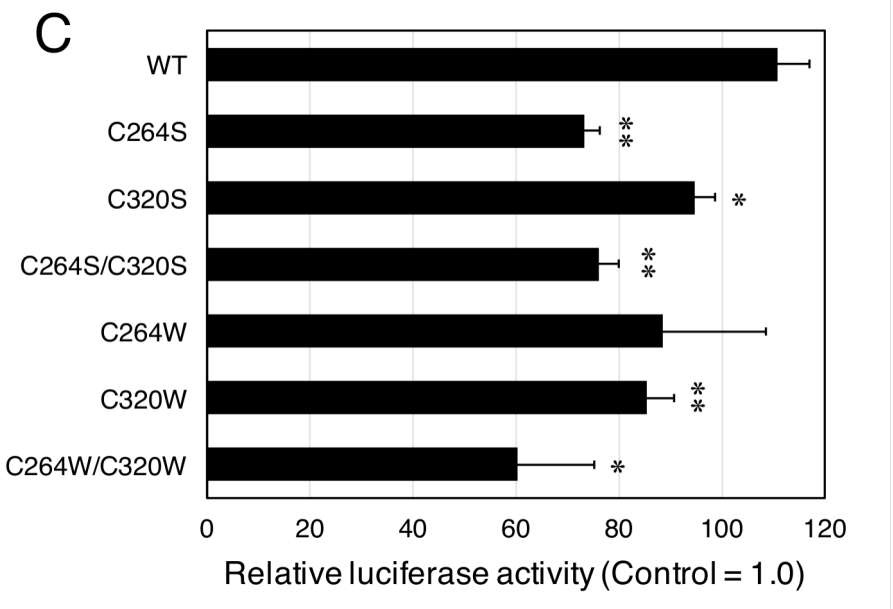

Figure 13. Continued

(C) Result of transient reporter assays to test effects of mutations at Csy-264 and Cys-320 of VND7 protein. Results were shown as relative values for the control effector (MCS = 1.0), and error bars indicate the SD (n=3). Asterisks indicate statistically significant differences (Welch's t-test; *P < 0.05, **P < 0.01) from the values for the wild type VND7 (WT).

Table 2. Summary of achieved conditions

Sample	Chromosome	Total no. of bases used	Mean Coverage
seiv1	1	1,747,764,211	×57.44
	2	1,658,110,707	×84.18
	3	1,930,750,189	×82.30
	4	1,161,910,717	×62.52
	5	1,634,854,069	×60.61
	All	8,133,389,893	×68.26
35S::VND7-VP16-GR	1	1,229,077,681	×40.39
	2	1,137,872,993	×57.77
	3	1,350,311,501	×57.56
	4	815,153,356	×43.86
	5	1,145,614,843	×42.47
	All	5,678,030,374	×47.66

Table 3. Summary of detected SNPs with whole genome sequencing

The Col-0 genome sequence on TAIR10 was used as a reference.

Chromosome	Sample	SNPs	Homo SNPs	Hetero SNPs
1	*seiv1*	844	63 (7.46%)	781 (92.54%)
	35S::VND7-VP16-GR	754	62 (8.22%)	692 (91.78%)
2	*seiv1*	984	121 (12.3%)	863 (87.7%)
	35S::VND7-VP16-GR	922	109 (11.82%)	813 (88.13%)
3	*seiv1*	818	129 (15.77%)	689 (84.23%)
	35S::VND7-VP16-GR	693	118 (17.03%)	575 (82.97%)
4	*seiv1*	918	127 (13.83%)	791 (86.17%)
	35S::VND7-VP16-GR	780	122 (15.64%)	658 (84.36%)
5	*seiv1*	1184	86 (7.26%)	1098 (92.74%)
	35S::VND7-VP16-GR	938	61 (6.5%)	877 (93.5%)
All	*seiv1*	4748	526 (11.08%)	4222 (88.92%)
	35S::VND7-VP16-GR	4087	472 (11.55%)	3615 (88.45%)

Table 4. Annotation of SNPs from the *seiv1*

Chromosome	Gene Symbol	Reference nucleotide	SNPs	Position in cDNA	Position in Protein	Amino Acid substitution
Chr5	AT5G39020	G	A	1537-1537	513-513	G->R
Chr5	AT5G40320	G	A	49-49	17-17	A->T
Chr5	AT5G42220	G	A	1137-1137	327-327	G->R
Chr5	AT5G42260	G	A	766-766	256-256	E->K
Chr5	AT5G42390	G	A	3100-3100	1015-1015	G->R
Chr5	AT5G42480	G	A	1360-1360	416-416	G->D
Chr5	AT5G42850	G	A	177-177	41-41	P->L
Chr5	AT5G43940	G	A	180-180	36-36	E->K
Chr5	AT5G44070	G	A	383-383	82-82	W->Stop
Chr5	AT5G44080	G	A	606-606	156-156	A->V
Chr5	AT5G45520	G	A	482-482	161-161	A->V
Chr5	AT5G45560	G	A	562-562	119-119	S->N
Chr5	AT5G48100	G	A	719-719	186-186	A->V
Chr5	AT5G48470	G	A	245-245	60-60	G->E
Chr5	AT5G49680	G	A	5206-5206	1736-1736	E->K

4. Discussion

4-1. GSNOR1-mediated NO metabolism regulation is critical for xylem vessel cell differentiation

In this work, I revealed that *seiv1*, the suppression mutant for xylem vessel cell differentiation, is a novel mutant allele of *GSNOR1* genes, functioning in the maintenance of cellular *S*-nitrosothiol homeostasis (Feechan et al., 2005; Lee et al., 2008; Airaki et al., 2011; Frungillo et al., 2014). Notably, the *seiv1* point mutant shared the reported phenotypes for loss-of-function *gsnor1* mutants, such as paraquat resistance (Fig. 6A; Chen et al., 2009) and increased cellular NO level (Fig. 6B; Lee et al., 2008; Chen et al., 2009). In *seiv1*, not only ectopic, but also endogenous xylem vessel cell differentiation was suppressed (Fig. 2B and Fig. 4). Similar abnormalities of vein formation in cotyledons, i.e. the discontinuous venation and vascular islands, were observed in both of *seiv1* and *gsnor1-3* (Fig. 9), indicating that GSNOR1-based NO metabolism is critical for xylem vessel cell formation. NO is one of highly active reactive nitrogen species (RNS), and the regulation of NO level is important for many cellular functions. The increased level of NO in *seiv1* (Fig. 6B) and in *gsnor1-3* (Feechan et al., 2005; Lee et al., 2008) suggest that higher level of NO has negative effects for xylem vessel cell formation. Especially, considering the observation that *seiv1* showed severe suppression of xylem vessel cell differentiation in above-ground organs, whereas the influences on transdifferentiation of root cells were mild (Fig. 2B), such effects of intracellular NO level on xylem vessel cell formation would be different in different xylem tissues in root and shoot.

4-2. Misregualtion of protein *S*-nitrosylation can affect xylem vessel cell differentiation

It is known that the states of protein *S*-nitrosylation were affected in *gsnor1-3* mutants (Hu et al., 2015), probably because of the disruption of normal *S*-nitrosothiol homeostasis. Few studies on effects of *S*-nitrosylation on protein activity are still limited (Spoel et al., 2010; Yu et al., 2014; Gibbs et al., 2015). However, *S*-nitrosylation of MC9, a metacaspase protein found preferentially in developing xylem and a direct regulatory target of VND7 (Yamaguchi et al., 2011). It was reported that *S*-nitrosylation of MC9 suppresses the autoprocessing during maturation of MC9 protein, as well as its proteolytic activity (Belenghi et al., 2007). Therefore, in *seiv1* and *gsnor1-3*, in which *S*-nitrosylation of MC9 apprears to be enhanced, MC9 activity may decrease, leading to the inhibition of xylem vessel cell differentiation. MC9 was not detected by the large-scale *S*-nitrosylation proteome analysis (Hu et al., 2015), suggesting the current large-scale proteome data is lacking the information of *S*-nitrosylation of cell type-specific proteins, such as differentiating xylem tracheary element cells, which only live for a

short time during development before PCD. Further utilization of the *35S-VND7:VP16:GR* and *seiv1* plants to *S*-nitrosylation proteome analysis should be promising strategy to obtain such information.

Protein *S*-nitrosylation in xylem vessel cell differentiation may also be related to auxin signaling. Auxin is known to be a critical factor for vascular cell development, including xylem vessel cell differentiation (reviewed by Miyashima et al., 2013). The core molecular mechanism of auxin signaling is rapid ubiquitin-mediated degradation of Aux/IAA transcriptional repressors, which inhibit the transcriptional activation activities of ARF transcription factors, through the action of the E3-ubiqutin ligase complex, $SCF^{TIR1/AFB}$ (Gray et al., 2001; Dharmasiri and Estelle, 2004). Auxin stabilizes the interaction between TIR1/AFB and Aux/IAA proteins, leading to the ubiquitination and degradation of Aux/IAA proteins (Dharmasiri et al., 2005; Kepinski and Leyser, 2005; Tan et al., 2007). Recently, Terrile et al. (2012) reported that *S*-nitrosylation of TIR1 protein can enhance the TIR1–Aux/IAA interaction, facilitating Aux/IAA degradation and subsequently promoting activation of gene expression by ARFs (Terrile et al., 2012). The ectopic *IAA2pro-GUS* expression was shown to be associated with the disconnected vein regions in *hyd1* mutant cotyledons (Pullen et al., 2010). According to these findings, the abnormal venation patterns in *seiv1* and *gsnor1-3* mutants may be explained, at least partly, by misregulation of TIR1 *S*-nitrosylation that result in aberrant auxin signaling.

Moreover, roles for GSNOR and *S*-nitrosylation can be considered from the viewpoint of this post-translational modification's relationship with other types of protein modification. Cysteine is known to be the targets of several kinds of reversible oxidative modifications, including *S*-nitrosylation, *S*-sulfenylation, *S*-glutathionylation, disulfide bonds, and *S*-acylation, in addition to irreversible modifications, such as sulphonic acid modification (Gu et al., 2002; Hogg, 2003; Hess et al., 2005; Paulsen and Carroll, 2013). It is possible that GSNOR-mediated protein *S*-nitrosylation regulation can function in the protection of cysteine residue from potentially toxic oxidative modifications, such as sulphonic acid modification (Gu et al., 2002; Hess et al., 2005). Interestingly, *S*-nitrosylation of histidine phosphotransfer protein AHP1, the important mediator of phosphate relay for cytokinin signaling, was reported to repress its phosphorylation and subsequent transfer of the phosphoryl group to its response regulator, ARR1 (Feng et al., 2013). The potential for crosstalk between *S*-nitrosylation and phosphorylation for the regulation of cell signaling suggests the hypothesis that in *seiv1* and *gsnor1-3* mutants, cytokinin signaling could be also affected. Detailed transcriptomic and *S*-nitrosylation proteomic observations of *seiv1* and *gsnor1-3* phenotypes would elucidate the impact of misregulation of protein *S*-nitrosylation for xylem vessel formation in the future.

4-3. VND7 is a target of the *S*-nitrosylation modification

Finally, I revealed that Cys-264 and Cys-320 residues of VND7 can be *S*-nitrosylated *in vitro*, based on the biotin-switch assay of recombinant VND7 protein experiments (Fig. 10-12). Because VND7 was not listed in the reported *S*-nitrosylation proteome data (Hu et al., 2015), my results provided a novel example of *S*-nitrosylated Arabidopsis protein. The possible *S*-nitrosylation target residues of VND7, Cys-264 and Cys-320, are localized closely to the transactivation domain, LP and WQ boxes (Fig. 12C; Yamaguchi et al., 2008). Quantitative RT-PCR data showed that the activation of VND7 downstream gene expressions was repressed in *seiv1* mutant (Fig. 3). Thus, it can be speculated that the increased *S*-nitrosylation level of VND7 at Cys-264 and/or Cys-320 could have inhibitory effects on VND7 transcriptional activation activity. Indeed, the transient reporter assay (Fig. 13) demonstrated that the transactivation activity of VND7 is decreased by the C264W/C320W mutations that may mimic *S*-nitrosylation (Feng et al., 2013). In consideration of the negative effects of GSNO application on VND7 transcriptional activation activity (Fig. 13B), the regulation of target gene expression by VND7 should be greatly disturbed in the *seiv1* mutant, where the NO level was increased (Fig. 6B). However, interestingly, I also found that the C264S and C320S mutations eliminating *S*-nitrosylation (Fig. 12C) affected the transactivation activity of VND7 (Fig. 13C). The latter finding would suggest that Cys-264 and Cys-320 are involved in the regulation of VND7 transactivation activity, through multiple types of Cys-based posttranslational modification, as discussed above.

It is suggestive that the Cys-320 residue of VND7, which possesses relatively high polarity (Fig. 12B), seems to be conserved in the other VND family proteins (Supplement Fig. 4), while Cys-264 is not. This may reflect different regulatory mechanisms for VND7 than the other family members. Further analysis should be carried out to make clear whether VND7 is *S*-nitrosylated *in vivo*, and roles of *S*-nitrosylation for regulation of VND family activities.

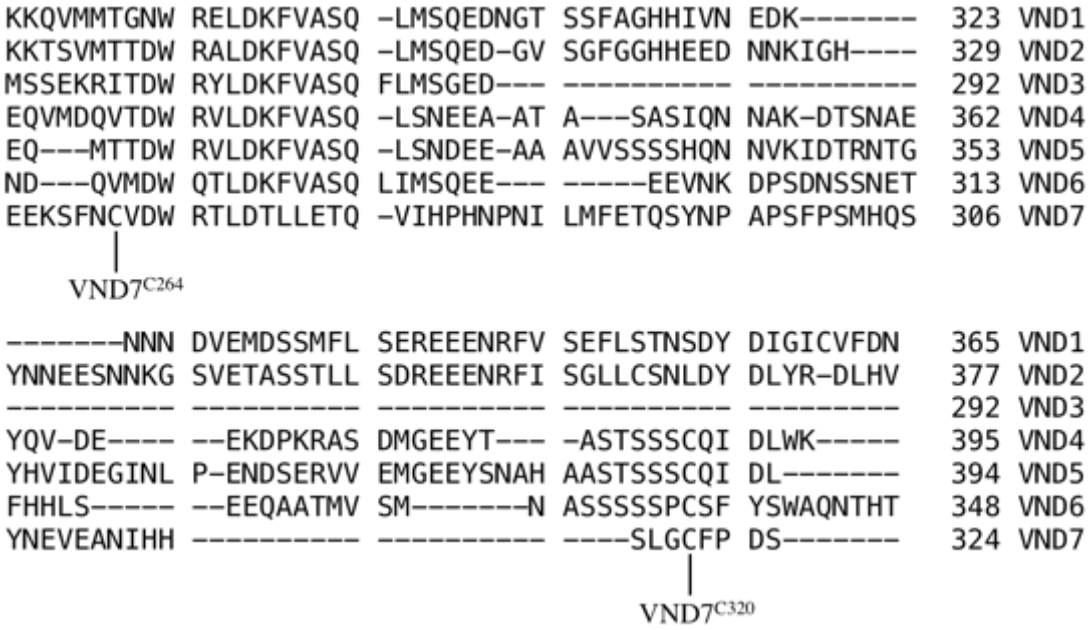

Supplement Figure 4. Partial alignment of amino acid sequences of VND family proteins

S-nitrosylation target of Cys-320 residue in VND7 protein, which possesses relatively high polarity (Fig. 12B), is conserved in the other VND family proteins, while C264 is not.

5. Acknowledgements

First and foremost, I would like to express my gratitude to my supervisor, Prof. Taku Demura. He has supported me with his immense knowledge, unsparing generosity, and zeal for my research project. His enthusiasm for scientific research and positive attitude to the life impacted me and will help me for my career in future. If it had not been for his support, I would never have done it. I also would like to thank the committee members, Prof. Masao Tasaka, Prof. Masaaki Umeda, for their invaluable advices and suggestions. Their guidance has served me well and I owe them my heartfelt appreciation.

I would like to thank Associate Prof. Masatoshi Yamaguchi for his encouragement and guidance. He has been a strong and supportive adviser to me throughout my doctoral course even after he had moved to Saitama University. I am also grateful to Assistant Prof. Misato Ohtani for her unstinted support and extraordinary knowledge. Her suggestion strongly encourages me and shows correct logical way. I thank Associate Prof. Ko Kato, Associate Prof. Minoru Kubo, and Assistant Prof. Arata Yoneda for their thoughtful mind and suggestion.

In addition, special thanks to Mr. Yoshito Ogawa, Dr. Hitoshi Endo, Dr. Yuto Takenaka, Mr. Taizo Tamura (NAIST), Ms. Ayumi Ihara, Ms. Arika Takebayashi, Ms. Ryoko Hiroyama, Ms. Tomoko Matsumoto, Ms. Akiko Sato, Ms. Kayo Kitaura (RIKEN) for their kind support of my experiment. All members of Metabolic Regulation of Plant Cells laboratory deserve my sincerest thanks, their friendship and assistance cannot be compared to anything.

Finally, I would like to thank sincerely my family; Masanori Kawabe, Chieko Kawabe, and Akinori Kawabe. They have been patient and supportive to me. I cannot express my geateful appreciation to them over.

6. References

1. Abel, S. and Theologis, A. (1994) Transient transformation of *Arabidopsis* leaf protoplasts: a versatile experimental system to study gene expression. *Plant J*. 5: 421−427.
2. Airaki M., Sánchez-Moreno L., Leterrier M., Barroso J. B., Palma J. M., and Corpas F. J. (2011). Detection and quantification of S-nitrosoglutathione (GSNO) in pepper (Capsicum annuum L.) plant organs by LC-ES/MS. *Plant Cell Physiol*. 52, 2006–2015.
3. Albertos P., Romero-Puertas M. C., Tatematsu K., Mateos I., Sánchez-Vicente I., Nambara E., et al. (2015). *S*-nitrosylation triggers ABI5 degradation to promote seed germination and seedling growth. *Nat. Commun*. 6, 8669.
4. Avci U., Petzold H. E., Ismail I. O., Beers E. P., and Haigler C. H. (2008) Cysteine proteases XCP1 and XCP2 aid micro-autolysis within the intact central vacuole during xylogenesis in Arabidopsis roots. *Plant J*. 56, 303–315.
5. Belenghi B., Romero-Puertas M.C., Vercammen D., Brackenier A., Inzé D., Delledonne M., Van Breusegem F. (2007) Metacaspase activity of *Arabidopsis thaliana* is regulated by *S*-nitrosylation of a critical cysteine residue. *J. Biol. Chem*. 282, (2), 1352-8.
6. Benhar, M., Forrester, M. T., and Stamler, J. S. (2009) Protein denitrosylation: enzymatic mechanisms and cellular functions. *Nat. Rev. Mol. Cell Biol*. 10, 721–732
7. Brown D. M., Zhang Z., Stephens E., Dupree P., and Turner S. R. (2009) Characterization of IRX10 and IRX10-like reveals an essential role in glucuronoxylan biosynthesis in Arabidopsis. *Plant J*. 57, 732–746.
8. Chen R., Sun S., Wang C., Li Y., Liang Y., An F., Li C., Dong H., Yang X., Zhang J., and Zuo J. (2009) The Arabidopsis PARAQUAT RESISTANT2 gene encodes an *S*-nitrosoglutathione reductase that is a key regulator of cell death. *Cell Res*. 19, 1377−1387.
9. Chiu J., March P.E., Lee R., Tillett D. (2004) Site-directed, Ligase-Independent Mutagenesis (SLIM): a single-tube methodology approaching 100% efficiency in 4 h. *Nucleic Acids Research* 32, e174.
10. Clough S.J. and Bent A.F. (1998) Floral dip: a simplified method for Agrobacterium-mediated transformation of Arabidopsis thaliana. *Plant J*. 16, 735-743.
11. Dharmasiri N., Dharmasiri S., and Estelle M. (2005) The F-box protein TIR1 is an auxin receptor. *Nature* 435, 441-445.
12. Endo H., Yamaguchi M., Tamura T., Nakano Y., Nishikubo N., Yoneda A., Kato K., Kubo M., Kajita S., Katayama Y., Ohtani M., Demura T. (2015) Multiple classes of transcription factors regulate the expression of *VASCULAR-RELATED NAC-DOMAIN7*, a master switch of xylem vessel differentiation. *Plant Cell Physiol*. 56, 242–254.

13. Ernst H.A., Olsen A.N., Larsen S., Lo Leggio L. (2004) Structure of the conserved domain of ANAC, a member of the NAC family of transcription factors. *EMBO Rep* 5, 297–303.
14. Escamez, S. and Tuominen, H. (2014) Programmes of cell death and autolysis in tracheary elements: when a suicidal cell arranges its own corpse removal. *J. Exp. Bot.* 65, 1313–1321.
15. Feechan A., Kwon E., Yun B.W., Wang Y., Pallas J.A., Loake G.J. (2005) A central role for *S*-nitrosothiols in plant disease resistance. *Proceedings of the National Academy of Sciences, USA* 102: 8054–8059.
16. Feng J., Wang C., Chen Q., Chen H., Ren B., Li X., Zuo J. (2013) *S*-nitrosylation of phosphotransfer proteins represses cytokinin signaling. *Nat. Commun* 4,1529.
17. Foster M.W., Forrester M.T., Stamler J.S. (2009) A protein microarray-based analysis of *S*-nitrosylation. *Proc. Natl. Acad. Sci. U S A.* 106, 18948–18953.
18. Frungillo L., Skelly M.J., Loake G.J., Spoel S.H., Salgado I. (2014) *S*-nitrosothiols regulate nitric oxide production and storage in plants through the nitrogen assimulation pathway. *Nature Communications* 5, 5401.
19. Fukuda H. (2004) Signals that control plant vascular cell differentiation. *Nature reviews molecular cell biology*, 5, 379-391.
20. Funk V., Kositsup B., Zhao C. and Beers E.P. (2002) The Arabidopsis xylem peptidase XCP1 is a tracheary element vacuolar protein that may be a papain ortholog. *Plant Physiol.* 128, 84–94.
21. Galli F., Rovidati S., Ghibelli L., Canestrari F. (1998) *S*-nitrosylation of glyceraldehyde-3-phosphate dehydrogenase decreases the enzyme affinity to the erythrocyte membrane. *Nitric Oxide* 2, 17–27.
22. Gibbs D.J., Conde J.V., Berckhan S., Prasad G., Mendiondo G.M., Holdsworth M.J. (2015) Group VII ethylene response factors coordinate oxygen and nitric oxide signal transduction and stress responses in plants. *Plant Physiol.*, 169, 23-31.
23. Gong B., Wen D., Wang X., Wei M., Yang F., Li, Y., Shi Q. (2015). *S*-nitrosoglutathione reductase-modulated redox signaling controls sodic alkaline stress responses in *Solanum lycopersicum L. Plant Cell Physiol.* 56, 790–802.
24. Gould N., Doulias P. T., Tenopoulou M., Raju K. and Ischiropoulos H. (2013) Regulation of Protein Function and Signaling by Reversible Cysteine *S*-Nitrosylation. *J. Biol. Chem.* 288, 26473–26479.
25. Gray, W. M., Kepinski, S., Rouse, D., Leyser, O. and Estelle, M. (2001). Auxin regulates SCF(TIR1)-dependent degradation of AUX/IAA proteins. Nature 414, 271-276.
26. Gu, Z., Kaul, M., Yan, B., Kridel, S.J., Cui, J., Strongin, A., Smith, J.W., Liddington, R.C., and Lipton, S.A. (2002). *S*-nitrosylation of matrix metalloproteinases: signaling pathway to

neuronal cell death. *Science* 297, 1186–1190.

27. Gupta K.J. (2011) Protein *S*-nitrosylation in plants: photorespiratory metabolism and NO signaling. *Sci. Signal.* 4, jc1
28. Hess, D.T., Matsumoto, A., Kim, S.O., Marshall, H.E., and Stamler, J.S. (2005) Protein S-nitrosylation: purview and parameters. *Nat. Rev. Mol. Cell Biol.*, 6, 150–166.
29. Hogg N. (2002) The biochemistry and physiology of *S*-nitrosothiols. *Annu. Rev. Pharmacol. Toxicol.* 42, 585–600.
30. Hogg, P. J. (2003) Disulfide bonds as switches for protein function. *Trends. Biochem. Sci.* 28, 210–214.
31. Hu J., Huang X., Chen L., Sun X., Lu C., Zhang L., Wang Y., Zuo J. (2015) Site-specific nitrosoproteomic identification of endogenously *S*-nitrosylated proteins in Arabidopsis. *Plant Physiol.*, 167: 1731–1746
32. J. S. Sperry (2003) Evolution of water transport and xylem structure. *Int. J. Plant Sci.* 164, (S3), S115–S127.
33. Jaffrey S.R., Erdjument-Bromage H., Ferris C.D., Tempst P., Snyder S.H. (2001) Protein *S*-nitrosylation: a physiological signal for neuronal nitric oxide. *Nat Cell Biol.* 3, 193–197.
34. Kepinski S., and Leyser O. (2005) The Arabidopsis F-box protein TIR1 is an auxin receptor. *Nature* 435, 446-451.
35. Kim, W. C., Ko J.H., Kim J.Y., Kim J., Bae H.J., Han K.H. (2013) MYB46 directly regulates the gene expression of secondary wall-associated cellulose synthases in Arabidopsis. *Plant J* 73, 26–36.
36. Kneeshaw S., Gelineau S., Tada Y., Loake G.J., Spoel S.H. (2014) Selective protein denitrosylation activity of Thioredoxin-h5 modulates plant Immunity. *Mol. Cell* 56, 153–162.
37. Kubienová L., Kopečný D., Tylichová M., Briozzo P., Skopalová J., Šebela M., Navrátil M., Tâche R., Luhová L., Barroso J.B., Petřivalský M. (2013) Structural and functional characterization of a plant *S*-nitrosoglutathione reductase from *Solanum lycopersicum*. *Biochimie* 95, 889–902.
38. Kubo M., Udagawa M., Nishikubo N., Horiguchi G., Yamaguchi M., Ito J., Mimura T., Fukuda H., Demura T. (2005) Transcription switches for protoxylem and metaxylem vessel formation. *Genes Dev.* 19, 1855–1860.
39. Kumar M., Campbell L., Turner S. (2016) Secondary cell walls: Biosynthesis and manipulation. *J. Exp. Bot.* 67, (2), 515–531.
40. Lee U., Wie C., Fernandez B.O., Feelisch M., Vierling E. (2008) Modulation of nitrosative stress by *S*-nitrosoglutathione reductase is critical for thermotolerance and plant growth in

Arabidopsis. *Plant Cell*, 20, 786-802.

41. Lin A. H., Wang Y. Q., Tang J. Y., Xue P., Li C. L., Liu L. C., Hu B., Yang F., Loake G.J., Chu C. (2012). Nitric oxide and protein *S*-nitrosylation are integral to hydrogen peroxide-induced leaf cell death in Rice. *Plant Physiol*. 158, 451–464.
42. Liu, L., Hausladen, A., Zeng, M., Que, L., Heitman, J., and Stamler, J. S. (2001) A metabolic enzyme for *S*-nitrosothiol conserved from bacteria to humans. *Nature* 410, 490–494.
43. Marino S.M., and Gladyshev V.N. (2010) Structural analysis of cysteine *S*-nitrosylation: A modified acid-based motif and the emerging role of trans-nitrosylation. *J Mol Biol* 395, (4), 844–859.
44. Miyashima S., Sebastian J., Lee J. Y. and Helariutta Y. (2013) Stem cell function during plant vascular development. *EMBO J*. 32, 178–193.
45. Nagata, T. (1987) Interaction of plant protoplast and liposome. *Methods Enzymol*. 148: 34–39.
46. Nakano Y., Yamaguchi M., Endo H., Rejab N.A., Ohtani M. (2015) NAC-MYB-based transcriptional regulation of secondary cell wall biosynthesis in land plants. *Front Plant Sci*. 6, 288.
47. Oda Y., and Fukuda H. (2012) Secondary cell wall patterning during xylem differentiation. *Curr. Opin*. *Plant Biol*., 15, 38-44.
48. Ohashi-Ito K., Oda Y., Fukuda H. (2010) Arabidopsis VASCULAR-RELATED NAC-DOMAIN6 directly regulates the genes that govern programmed cell death and secondary wall formation during xylem differentiation. *Plant Cell* 22, 3461–73.
49. Paulsen, C. E. and Carroll, K. S. (2013) Cysteine-Mediated Redox Signaling: Chemistry, Biology, and Tools for Discovery. *Chem*. *Rev*. 113, 4633–4679.
50. Persson S., Caffall K.H., Freshour G., Hilley M.T., Bauer S., Poindexter P., Hahn M.G., Mohnen D., Somerville C. (2007) The *Arabidopsis irregular xylem8* mutant is deficient in glucuronoxylan and homogalacturonan, which are essential for secondary cell wall integrity. *Plant Cell* 19, (1), 237-55.
51. Pullen M., Clark N., Zarinkamar F., Topping J., Lindsey K. (2010) Analysis of vascular development in the hydra sterol biosynthetic mutants of Arabidopsis. *PLoS ONE* 5, e12227
52. Schuetz M., Smith R., and Ellis B. (2013) Xylem tissue specification, patterning, and differentiation mechanisms. *J*. *Exp*. *Bot*., 64, 11-31.
53. Shi Y.F., Wang D.L., Wang C., Culler A.H., Kreiser M.A., Suresh J., Cohen J.D., Pan J.W., Baker B., Liu J.Z. (2015) Loss of GSNOR1 function leads to compromised auxin signaling and polar auxin transport. *Molecular Plant* 8, 1350–1365.
54. Skelly M.J., Frungillo L., Spoel S.H. (2016) Transcriptional regulation by complex

interplay between post-translational modifications. *Curr. Opin. Plant Biol.* 33, 126-132

55. Snider N. T. and Omary M. B. (2014) Post-translational modifications of intermediate filament proteins: mechanisms and functions. *Nat. Rev. Mol. Cell Biol.* 15, 163–177.
56. Soyano, T., Thitamadee, S., Machida, Y., Chua, N.H. (2008). ASYMMETRIC LEAVES2-LIKE19/LATERAL ORGAN BOUNDARIES DOMAIN30 and ASL20/LBD18 regulate tracheary element differentiation in Arabidopsis. *Plant Cell* 20, 3359–3373.
57. Sperry J.S. (2003). Evolution of water transport and xylem structure. *International Journal of Plant Science* 164: S115-S127.
58. Spoel S.H. and Loake G.J. (2011) Redox-based protein modifications: the missing link in plant immune sigalling. *Curr. Opin. Plant Biol.* 14, 358-364.
59. Spoel, S.H., Tada, Y., and Loake, G.J. (2010). Post-translational protein modification as a tool for transcription reprogramming. *New Phytol.*, 186, 333–339.
60. Structural Genomics Consortium, China Structural Genomics Consortium, Northeast Structural Genomics Consortium, Gräslund, S., Nordlund, P., Weigelt, J., Hallberg, B. M., Bray, J., Gileadi, O., Knapp, S., Oppermann, U., Arrowsmith, C., Hui, R., Ming, J., dhe-Paganon, S., et al. (2008) Protein production and purification. *Nat. Methods* 5, 135–146.
61. Tada Y., Spoel S.H., Pajerowska-Mukhtar K., Mou Z., Song J., Wang C., Zuo J., Dong X. (2008) Plant immunity requires conformational changes of NPR1 via *S*-nitrosylation and thioredoxins. *Science* 321, 952–956.
62. Tan X., Calderon-Villalobos L.I., Sharon M., Zheng C., Robinson C.V., Estelle M. and Zheng N. (2007) Mechanism of auxin perception by the TIR1 ubiquitin ligase. *Nature* 446, 640–645.
63. Taylor N.G., Howells R.M., Huttly A.K., Vickers K. and Turner S.R. (2003) Interactions among three distinct CesA proteins essential for cellulose synthesis. *Proc. Natl Acad. Sci. USA* 100, 1450–1455.
64. Terrile M.C., Paris R., Calderon-Villalobos L.I., Iglesias M.J., Lamattina L., Estelle M., et al. (2012) Nitric oxide influences auxin signaling through *S*-nitrosylation of the Arabidopsis TRANSPORT INHIBITOR RESPONSE 1 auxin receptor. *Plant J.* 70, (3), 492–500.
65. Turner S., Gallois P., Brown D. (2007) Tracheary element differentiation. *Annual Review of Plant Biology* 58, 407–433.
66. Wang P., Du Y., Hou Y.J., Zhao Y., Hsu C.C., Yuan F., Zhu X., Tao W.A., Song C.P., Zhu J.K. (2015) Nitric oxide negatively regulates abscisic acid signaling in guard cells by *S*-nitrosylation of OST1. *Proc Natl Acad Sci U S A.* 112, (2), 613–8.
67. Wang X., Kettenhofen N.J., Shiva S., Hogg N., and Gladwin M.T. (2008) Copper dependence of the biotin switch assay: modified assay for measuring cellular and blood

nitrosated proteins. *Free Radic. Biol. Med.* 44, 1362–1372.

68. Wang Y.C., Peterson S.E., Loring J.F. (2014) Protein post-translational modifications and regulation of pluripotency in human stem cells. *Cell Res.* 24, 143–160.
69. Wendehenne D., Pugin A., Klessig D.F., Durner J. (2001) Nitric oxide: comparative synthesis and signaling in animal and plant cells. *Trends Plant Sci.* 6, 177–183.
70. Xu B., Ohtani M., Yamaguchi M., Toyooka K., Wakazaki M., Sato M., Kubo M., Nakano Y., Sano R., Hiwatashi Y., Murata T., Kurata T., Yoneda A., Kato K., Hasebe M., Demura T. (2014) Contribution of NAC transcription factors to plant adaptation to land. *Science* 343, 1505-1508
71. Xu S., Guerra D., Lee U., and Vierling E. (2013) *S*-nitrosoglutathione reductases are low-copy number, cysteine-rich proteins in plants that control multiple developmental and defense responses in Arabidopsis. *Front. Plant Sci.* 4, 430.
72. Yamaguchi M., Goué N., Igarashi H., Ohtani M., Nakano Y., Mortimer J.C., Nishikubo N., Kubo M., Katayama Y., Kakegawa K., Dupree P., Demura T. (2010) *VASCULAR-RELATED NAC-DOMAIN6* and *VASCULAR-RELATED NAC-DOMAIN7* effectively induce transdifferentiation into xylem vessel elements under control of an induction system. *Plant Physiol.* 153(3), 906–914.
73. Yamaguchi M., Kubo M., Fukuda H., Demura T. (2008) *VASCULAR-RELATED NAC-DOMAIN7* is involved in differentiation of all types of xylem vessels in Arabidopsis roots and shoots. *Plant J.* 55, 652-664.
74. Yamaguchi M., Mitsuda N., Ohtani M., Ohme-Takagi M., Kato K., Demura T. (2011) *VASCULAR-RELATED NAC-DOMAIN7* directly regulates the expression of a broad range of genes for xylem vessel formation. *Plant J.* 66, 579–590.
75. Yamaguchi M., Ohtani M., Mitsuda N., Kubo M., Ohme-Takagi M., Fukuda H., Demura T. (2010) *VND-INTERACTING2*, a NAC domain transcription factor, negatively regulates xylem vessel formation in Arabidopsis. *Plant Cell* 22, 1249–1263.
76. Yazaki J., Galli M., Kim A.Y., Nito K., Aleman F., Chang K.N., Carvunis A.R., Quan R., Nguyen H., Song L., Alvarez J.M., Huang S.S., Chen H., Ramachandran N., Altmann S., Gutiérrez R.A., Hill D.E., Schroeder J.I., Chory J., LaBaer J., Vidal M., Braun P., Ecker J.R. (2016) Mapping transcription factor interactome networks using HaloTag protein arrays. *Proc. Natl. Acad. Sci. USA* 113, (29), 4238-47.
77. Yu M., Lamattina L., Spoel S.H., Loake G.J. (2014) Nitric oxide function in plant biology: a redox cue in deconvolution. *New Phytol.*, 202, 1142–1156.
78. Yun B.W., Feechan A., Yin M., Saidi N.B., Le Bihan T., Yu M., Moore J.W., Kang J.G., Kwon E., Spoel S.H., Pallas J.A., Loake G.J. (2011). *S*-nitrosylation of NADPH oxidase

regulates cell death in plant immunity. *Nature* 478, 264–268.

79. Zaffagnini M., Fermani S., Costa A., Lemaire S.D., Trost P. (2013) Plant cytoplasmic GAPDH: redox post-translational modifications and moonlighting properties. *Front Plant Sci*. 4, 450.
80. Zhong R. and Ye Z.H. (2015) Secondary cell walls: biosynthesis, patterned deposition and transcriptional regulation. *Plant Cell Physiol*. 56, 195– 214.
81. Zhong R. J., Lee C. and Ye Z.-H. (2010) Global analysis of direct targets of secondary wall NAC master switches in Arabidopsis. *Molecular Plant* 3, 1087–1103.
82. Zhou J., Zhong R., Ye Z.H. (2014) Arabidopsis NAC domain proteins, VND1 to VND5, are transcriptional regulators of secondary wall biosynthesis in vessels. *PLoS ONE*. 9, e105726.
83. Zor T., and Selinger Z. (1996) Linearization of the Bradford protein assay increases its sensitivity: theoretical and experimental studies. *Anal. Biochem* 236, 302–308.